Pergamon

Journal of Structural Geology, Vol. 17, No. 2, pp. 163 to 182, 1995

0191-8141/95 $9.50+0.00

0191-8141(94)E0042-W

Syn-collisional extensional collapse parallel to the orogenic trend in a domain of steep tectonics: the Salamanca Detachment Zone (Central Iberian Zone, Spain)

M. A. DIEZ BALDA, J. R. MARTINEZ CATALAN and P. AYARZA ARRIBAS

Departamento de Geología, Facultad de Ciencias, Universidad de Salamanca, 37008 Salamanca, Spain

(*Received* 1 *November* 1993; *accepted in revised form* 16 *March* 1994)

Abstract—The area south of the town of Salamanca is a zone of the Spanish Variscan Belt characterized by a first compressional event which gave rise to steep structures, followed by the development of an extensional ductile shear zone, more than 4 km thick, that is described as the Salamanca Detachment Zone. The strain associated to the detachment is analyzed using quartz pebbles in conglomerates. Comparing the measured strain values with theoretical strain paths, leads to the conclusion that the deformation was approximately of plane strain type. Quartz *c*-axis fabrics and kinematic criteria indicate that simple shear was a very important component of the deformation, though coaxial components were probably involved. The extensional character of the detachment is indicated by the geometry of the metamorphic zones and the metamorphic evolution.

Taken together, the data indicate that the extensional event was related to gravitational collapse induced by the thickening of the continental crust, and that it was syn-collisional. The movement of the hangingwall unit was to the southeast, parallel to the trend of the fold belt, and the translation was of the order of one to a few dozens of km. Though important, this is not exceedingly large, and allowed the preservation of low-grade metamorphic conditions in the hangingwall, preventing it from being affected by extensive brittle tectonic processes.

INTRODUCTION

The Central Iberian Zone (CIZ) occupies the central part of the Iberian Massif (Fig. 1), which is the southern branch of the Ibero-Armorican Arc, in the Variscan Belt of Western Europe. It is an internal zone of the orogen and also the largest of the zones into which the Iberian Massif has been divided (Julivert *et al.* 1972). The CIZ is characterized by its stratigraphy, consisting of thick pre-Ordovician terrigenous sequences (mainly Upper Proterozoic and Lower Cambrian) and by the transgressive character of the Lower Ordovician quartzite (Julivert *et al.* 1972). Also characteristic is the existence of huge amounts of pre-Variscan, felsic volcanic and plutonic rocks, outcropping mainly in its eastern and northern parts.

Prior to the Variscan deformation, the zone was affected by the Cadomian Orogeny and by Lower Paleozoic tectonics, mainly of extensional type, though a phase of inversion by dextral transpression has been mentioned between the Cambrian and the Ordovician by Lefort & Ribeiro (1980). These tectonic effects can be seen in the felsic vulcanism and granitic plutonism of Late Proterozoic and Early Paleozoic age and in the existence of folding and unconformities of the same ages.

The Variscan structure of the CIZ consists of the superposition of several syn-metamorphic deformation episodes, mostly compressive, which gave rise to an important crustal thickening in some areas. Differences in the geometry of the first phase folds allowed Díez Balda *et al.* (1990) to distinguish two structural domains in the CIZ: the Domain of Recumbent Folds to the east and north, and the Domain of Vertical Folds to the south (Fig. 1), though areas with inclined and even recumbent folds also exist locally in the second domain (Ribeiro *et al.* 1990).

In the first domain the thickening was achieved by the development of huge recumbent folds, the cores of which are often occupied by orthogneisses, and by the stacking of thrust sheets along sub-horizontal ductile shear zones, which involve the orthogneissic basement (Macaya *et al.* 1991). This is interpreted as the result of crustal-scale sub-horizontal simple shear. Conversely, in the Domain of Vertical Folds, characterized by very continuous but not strongly flattened folds, with sub-vertical axial surfaces and sub-horizontal axes, the thickening was probably achieved by a different type of tectonics. It could simply be a coaxial mechanism, with horizontal shortening normal to the trend of the belt and lengthening in the vertical and in the horizontal direction parallel to the trend. However, the clockwise transection of both limbs of the folds by the first cleavage in some of the major folds suggests a component of distributed simple shear related to transcurrent movements (Aller *et al.* 1986, Dias & Ribeiro 1991 a,b). The transition from one domain to the other is obscured by the presence of huge amounts of Variscan granitoids.

The study area, south of Salamanca, is in the Domain of Vertical Folds and is well suited for the analysis of the structural evolution, due to the exposure of rocks from different structural levels. The succession consists of a thick sequence of Upper Proterozoic age, and an incomplete Paleozoic sequence. They were deformed in

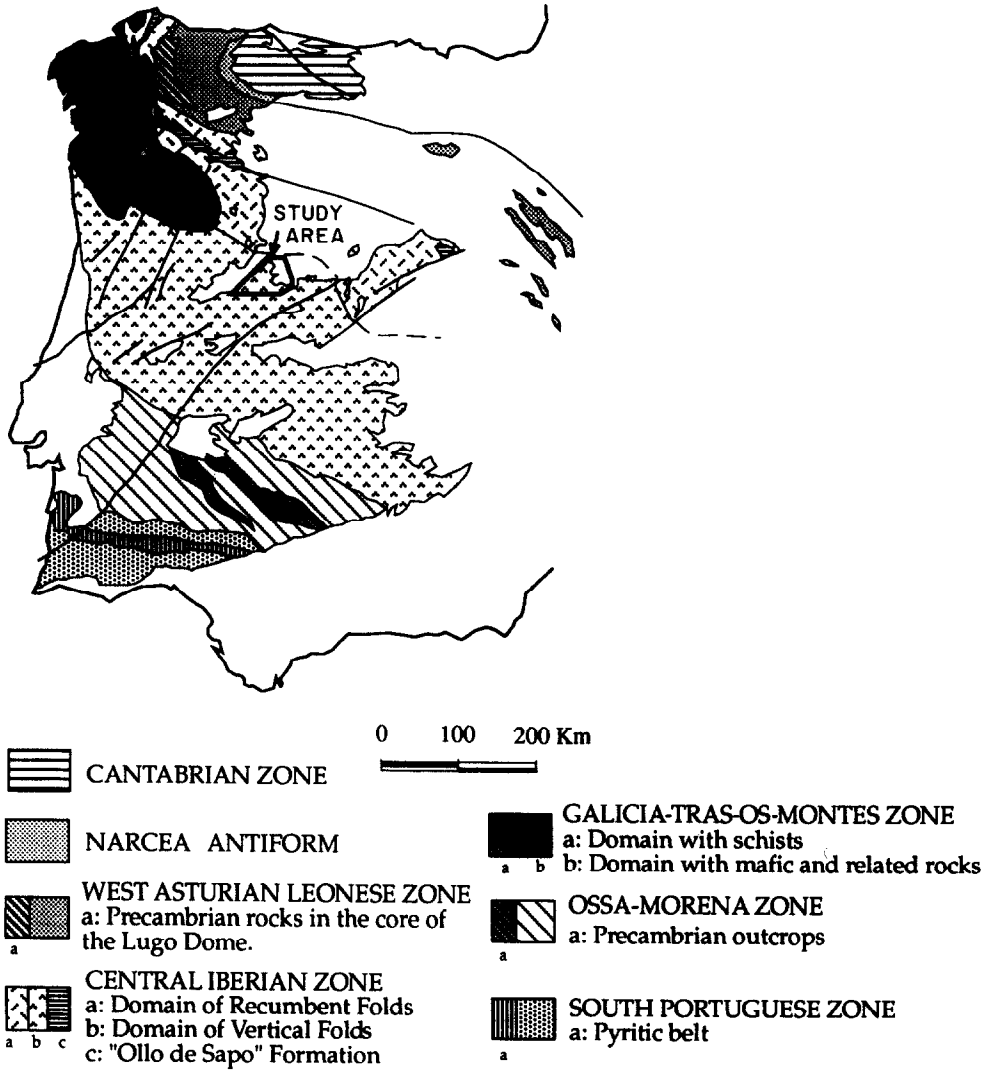

Fig. 1. Subdivision in zones of the Iberian Massif, modified from Julivert *et al.* (1972), showing the location of the area studied.

Variscan times by three main deformation episodes. The first deformation phase, D_1, affected all the rocks and all the structural levels, giving rise to kilometre-scale folds with sub-vertical axial surfaces and a pervasive axial planar cleavage, S_1. The second phase, D_2, developed a sub-horizontal penetrative foliation, S_2, in the low structural levels as well as minor folds and other structures indicative of an important component of rotational deformation. Pre-Variscan granitoids were mylonitized and Variscan granites, emplaced during this event, were heterogeneously deformed. The third phase, D_3, produced open vertical folds with a very large wavelength and small amplitude. These folds bend the metamorphic isograds and the foliated granitic rocks.

This work deals with the structural and metamorphic analysis of the region south of Salamanca during the Variscan Orogeny, focusing on the superposition of strains of the first two deformation events and on the strain regime, kinematics and tectonic significance of the second event.

GEOLOGICAL SETTING: STRATIGRAPHY, METAMORPHISM AND PLUTONIC ROCKS

The oldest sedimentary rocks outcropping in the area are a group of monotonous terrigenous sediments of Upper Proterozoic age, the Schist–Greywacke Complex. Díez Balda (1981, 1986) distinguished two formations in this complex (Fig. 2). The lower one, called the Monterrubio Formation, consists of more than 2000 m of mainly pelitic rocks, with thin layers of conglomerates, sandstones and felsic volcanoclastics. The Aldeatejada Formation overlies conformably the previous one and consists of more than 2500 m of slates, mudstones and siltstones, with minor alternations of sandstones and some lenticular bodies of gravity-deposited brecciated limestones and pebbly mudstones. The age of the Aldeatejada Formation is considered Late Vendian, that is, uppermost Proterozoic (Palacios & Vidal 1992).

The Aldeatejada Formation grades upwards to the Tamames Sandstone, a sub-tidal shelf succession, 650 m

thick, made up of sandstones and pelites where Lower Cambrian trilobites have been found (García de Figuerola & Martínez García 1972). Above this, the Tamames Limestone, with a thickness ranging from 150 to 650 m, is also of Lower Cambrian age (Perejón 1972) and, locally, an unfossiliferous pelitic formation, the Endrinal Slates, probably of Lower Cambrian age, overlies the limestone.

The Lower Ordovician rests unconformably on older formations (Fig. 3). The basal formation is a very continuous and competent horizon known as the Armorican Quartzite, of Arenig age, and consists of an alternation of 300 m of quartzites, sandstones and slates representing a sub-tidal shelf environment. It is conformably overlain by La Bastida Slates, with a thickness of 600 m and an age ranging from Lower Llanvirn to Lower Llandeilo (Jiménez Fuentes 1982, Gutiérrez Marco & Rábano 1983). The Silurian rocks crop out only in the core of the Tamames Syncline and consist of some 700 m of detrital rocks alternating with mafic volcanics (Díez Balda 1986), ranging in age from Lower Llandovery to Lower Ludlow (Rölz 1975, Gutiérrez Marco & Rábano 1983).

The Variscan deformation was accompanied by a regional metamorphism in which two stages can be distinguished: a first stage of Barrovian type, i.e. of intermediate pressure and with associations of staurolite and almandine, followed by a low pressure stage in which cordierite and andalusite developed. The change to lower pressure conditions occurred during the second deformation event and was probably isothermal, the sillimanite being stable in the deepest areas presently outcropping, where migmatization conditions were reached.

Plutonic rocks are abundant, and a division can be established between deformed and non-deformed rocks. The former are a group of pre-Variscan orthogneisses and Variscan deformed granites outcropping in the cores of late open antiforms and in the southeast of the area, i.e. from deep structural levels (Figs. 2, 3 and 4). The non-penetratively deformed granitoids are Late Variscan rocks cross-cutting the D_1 and D_2 structures of the country rock. They outcrop mainly in the *S* as a large pluton of biotitic granodiorites, and also as small discordant bodies (Figs. 2 and 4) and are considered to be syn- to post-D_3 intrusions.

THE VARISCAN DEFORMATION

Pre-Variscan events are identified by the unconformity at the base of the Armorican Quartzite and also by the variable plunge shown by the L_1 intersection lineation in pre-Ordovician metasediments. It is assumed that folding and tilting occurred in pre-Ordovician times, related to the Cadomian Orogeny, Lower Paleozoic extension and episodic tectonic inversions. However, these episodes did not give rise to appreciable internal deformation in the rocks and no relics of Cadomian or pre-Variscan metamorphism have been identified in the area. All of the structures and the internal deformation shown by the Proterozoic and Cambrian rocks are also present in the Ordovician and Silurian rocks and are described below.

The first deformation phase (D_1)

The first Variscan episode produced a regular train of folds with sub-vertical axial surfaces striking NW–SE, well developed in the pre-Ordovician rocks (Figs. 2 and 3). The wavelengths range between 3 and 5 km and the amplitudes from 0.5 to 2 km. The Ordovician and Silurian rocks, due to the presence of the competent Armorican Quartzite, developed somewhat larger folds, with wavelengths of more than 10 km and amplitudes of up to 4 km, which are a characteristic element in the landscape of the whole Domain of Vertical Folds.

A penetrative slaty cleavage, S_1, axial planar to the folds, is very well developed in pelitic lithologies and has been preserved in the low-grade metamorphic areas (chlorite and biotite zones). In the sandstones it is often a rough cleavage and may be a spaced cleavage in the quartzites. The fold hinges and the intersection lineations between the layering and the S_1 cleavage are subhorizontal in most cases, though they can plunge up to 90° in the pre-Ordovician rocks due to interference with pre-Variscan folding or tilting.

The D_1 *strain ellipsoid.*The internal deformation of the first episode has been evaluated in outcrops of the chlorite zone, where post-D_1 superimposed deformation is negligible. The pre-tectonic strain markers used were dolomitic nodules in slates, and quartz pebbles in monomictic conglomerates with very low matrix content. The method applied was the R_f/Φ technique (Ramsay 1967, Dunnet 1969, Lisle 1985), and in both lithologies it has been assumed that deformation was homogeneous at the outcrop or sample scale, the behaviour of the markers was passive and the ductility contrast between the markers and the matrix is negligible, which is reasonable as there are no pressure shadows around the dolomitic nodules and the matrix content in the conglomerates is insignificant.

The samples were cut along three orthogonal planes that were assumed to be the principal planes of the strain ellipsoid, deduced from the cleavage and the stretching lineation. The latter is marked by quartz fibres in pressure shadows or, approximately, by the statistically preferred orientation of the longest dimension of pre-tectonic objects. As the cleavage is always visible, the *XY* plane was often cut and measured first, the orientation of the *X* axis was deduced and then the *XZ* and *YZ* planes were cut and measured. The data were then plotted in a R_f/Φ diagram and adjusted with the curves of different initial shape values, R_i. Also, the equations of Lisle (1985, pp. 3–7 and p. 14) were used to calculate the R_s values that allowed a best-fit of the points, as well as the vector mean and the harmonic mean of the R_f values for each distribution, to apply a symmetry test. The strain data were plotted in a Flinn diagram (Fig. 5).

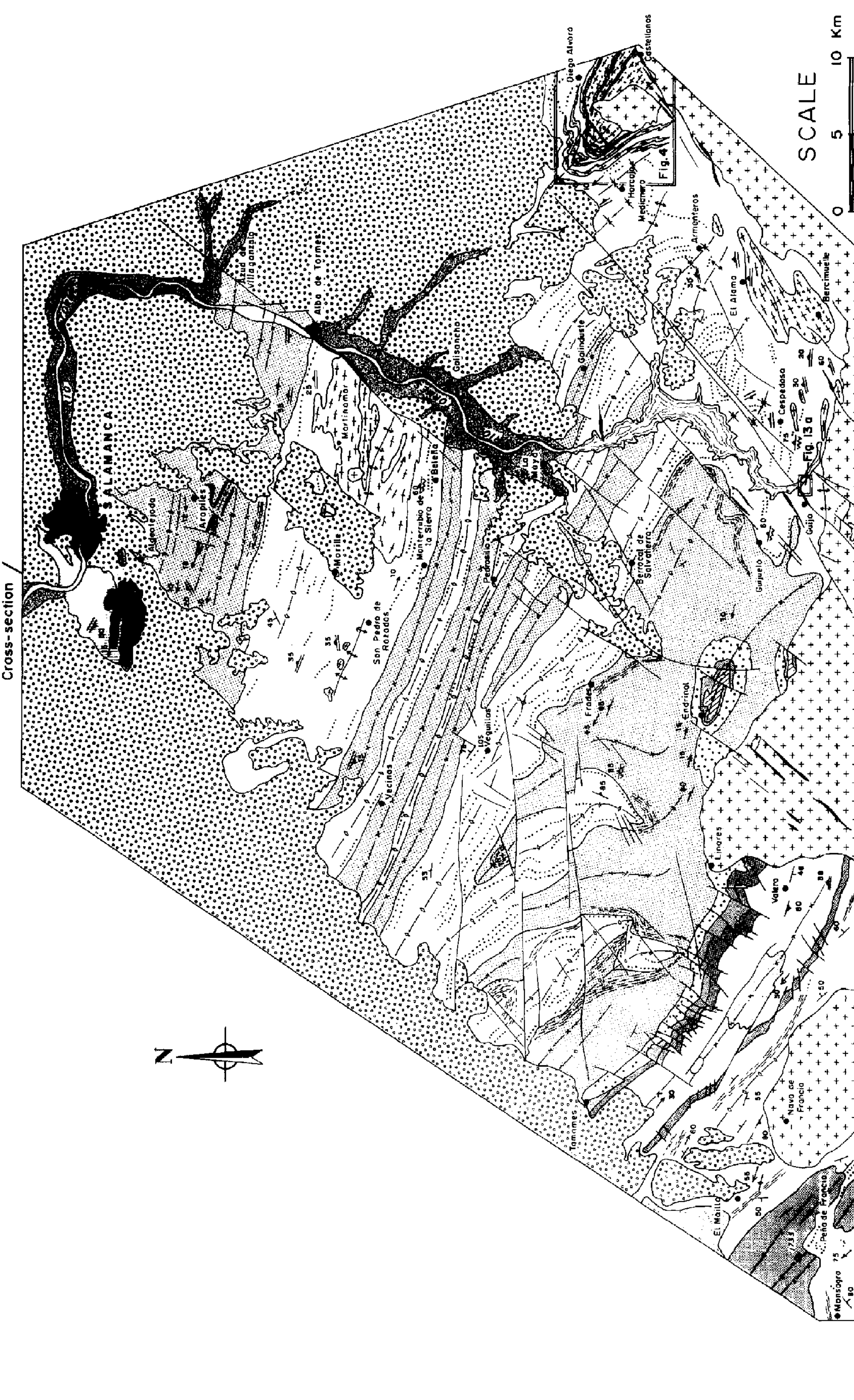
Cross-section
SALAMANCA
Alba de Tormes
Aldeatejada
Arapiles
Morille
Martinamor
Monterrubio de la Sierra
Beleña
Galisancho
Pedrosillo
San Pedro de Rozados
Vecinos
Veguillas
Frades
Endrinal
Berrocal de Salvatierra
Guijuelo
Guijo
Cespedosa
El Alamo
Armenteros
Bercimuelle
Horcajo
Medinero
Diego Alvaro
Castellanos
Fig. 4
Fig. 13a
Linares
Valero
Tamames
Nava de Francia
El Maillo
Peña de Francia
Monsagro
SCALE
0 5 10 Km
N

Fig. 2.

Two outcrops of slates with dolomitic nodules belonging to the Aldeatejada Formation, were analyzed. For the first, in Azud de Villagonzalo (Figs. 6 and 7a; see Fig. 2 for location), the following axial ratios were measured for the strain ellipsoid (samples AZ1 and AZ2, see Fig. 5): $X/Y = 2.5$ and 2.6, $Y/Z \doteq 5.7$ and 5.8, $X/Z = 13$ and 15, with a k value (Flinn, 1962) of 0.32 and 0.33. The strike of the XY plane is 100° vertical, as is the well-developed slaty cleavage, and the X axis is horizontal. For the second outcrop, southwest of Arapiles (AP), the results are: $X/Y = 2.3$, $Y/Z = 4.7$, $X/Z = 11.4$ and $k = 0.35$, the XY plane having the same orientation and the X axis plunging 13°W.

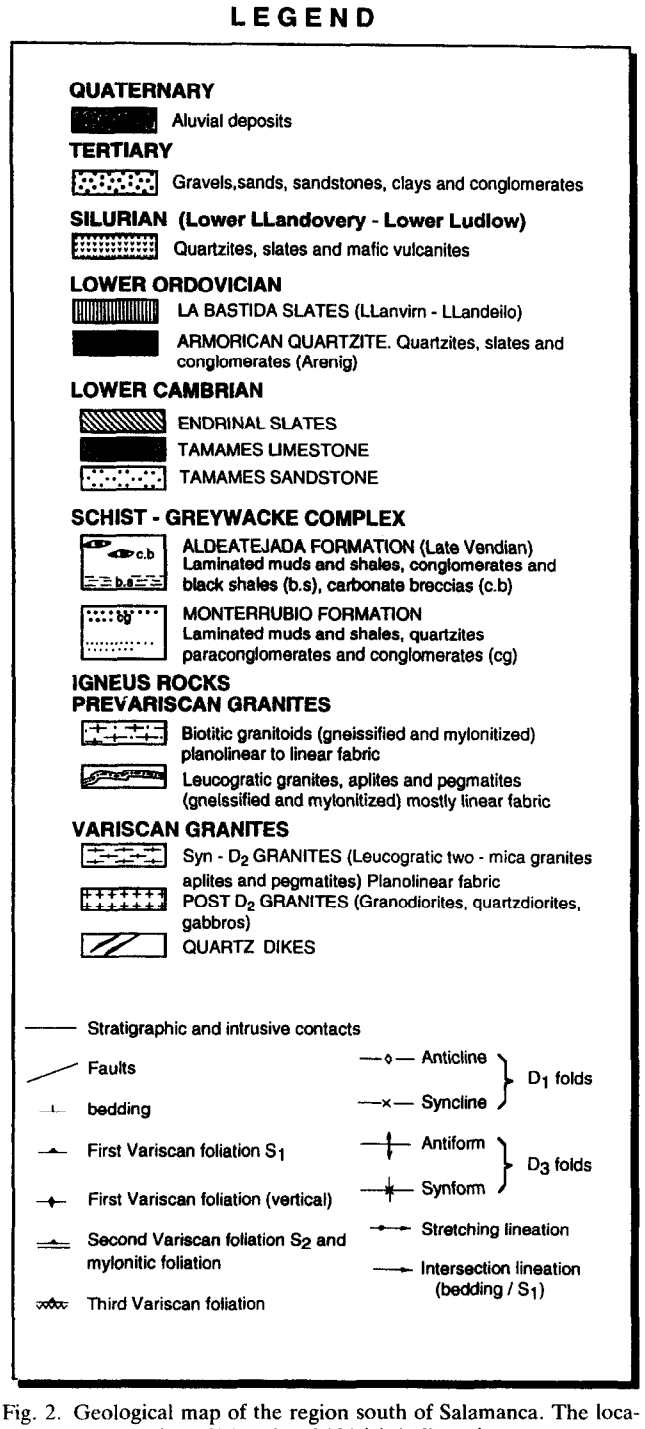

Fig. 2. Geological map of the region south of Salamanca. The location of Figs. 4 and 13(a) is indicated.

Quartzitic conglomerates, intercalated in the Monterrubio Formation, were analyzed in the localities (Fig. 2) of Frades (FR1 and FR2) and Berrocal de Salvatierra (BS1 and BS2). The results (Fig. 5) give the following values (Fig. 8a): $X/Y = 1.7$ to 1.9, $Y/Z = 1.5$ to 1.8, $X/Z = 2.7$ to 3.3 and $k = 0.8$ to 1.7, with the XY plane striking 130° and dipping 70–80°N and the X axis plunging 10°NW.

The R_f/Φ patterns obtained (Figs. 6 and 8a) are quite symmetric, so that the initial fabrics are considered to have been random or to have been symmetric and then subjected to strains imposed in a symmetrical fashion. The indexes of symmetry (I_{SYM} in the figures), as defined by Lisle (1985), are greater than the critical values reported by this author for the number of objects and R_s values measured in each case. The existence of points in the interior of the curves indicates that the objects were originally elliptical and had variable initial axial ratios.

The results indicate that the region was shortened during the D_1 event in the direction NE–SW, normal to the trend of the fold belt, and that the maximum elongation was in the horizontal direction parallel to the fold axes. The flattening was more important in the slaty lithologies, where the ellipsoids plot in the field of apparent flattening ($k = 0.32$–0.35), whereas in the conglomerates it is close to the apparent plane strain type ($k = 0.8$, 1.1, 1.2 and 1.7). For the conglomerates, which are the most important lithologies in the following discussion, no significant volume loss seems to have taken place, as pressure solution indicators are absent or very scarce.

The deformation could have been achieved by pure shear or by more complex strain histories involving pure and simple shear. Work done on D_1 folds of other areas of the CIZ and based on the transection of both limbs by the S_1 cleavage (Almadén Syncline, Aller *et al.* 1986), on the different attitude of the stretching lineation in both limbs of the folds (Valongo Anticline, Dias & Ribeiro 1991a), or on the different reorientation of burrows initially normal to the bedding in both limbs (Moncorvo Syncline, Dias & Ribeiro 1991b), suggests a transcurrent movement component of sinistral type. A mechanism of sinistral transpression (Sanderson & Marchini 1984) has consequently been proposed (Dias & Ribeiro 1991a,b), and is in accordance with the fact that the most probable age for the D_1 event in the CIZ is Upper Devonian–Lower Carboniferous (Ribeiro *et al.* 1990), the same as for the activity of the sinistral Badajoz-Córdoba Shear Zone in the southern boundary of the CIZ (Burg *et al.* 1981, Chacón *et al.* 1983, García Casquero *et al.* 1988, Dallmeyer & Quesada 1989).

The second deformation phase (D_2)

The distribution of D_2 structures is closely related to the Barrovian metamorphic zonation. Structurally above the almandine zone, the Barrovian gradient is normal, with a chlorite zone several km thick and a biotite zone of around 2 km (Fig. 3). In the large areas corresponding to these two zones (Fig. 9), folds with

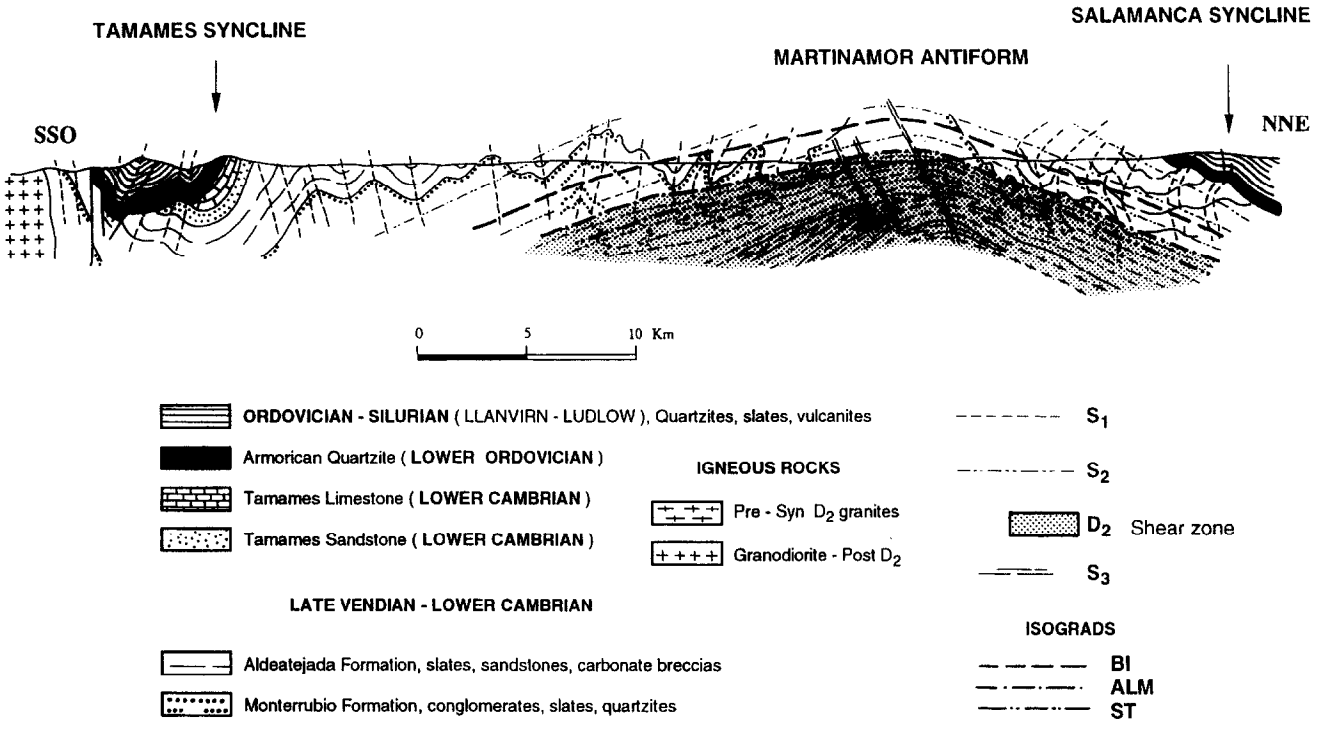

Fig. 3. Geological cross-section of the study area. The D_2 detachment zone, which is folded by the Martinamor Antiform, is shown in a section perpendicular to the shear direction. Note the open folds, with sub-horizontal axial surface, affecting the S_1 cleavage above the shear zone. For location, see Fig. 2.

sub-horizontal axial surfaces and related crenulation cleavages are developed. D_2 minor folds are often angular and open, with interlimb angles between 80 and 110° (Fig. 10a). Some major angular folds exist, producing open sub-horizontal flexures in the S_1 cleavage to the scale of the outcrop and also of the cross-section (Fig. 3).

Internal deformation in these areas is indicated by a sub-horizontal fabric in the slates, which varies from an irregularly distributed and non-pervasive spaced cleavage or crenulation in the chlorite zone to a more regular and pervasive crenulation cleavage in the biotite zone. In the former zone, the accumulation of oxides in the S_2 surfaces points to a component of pressure solution in its genesis. In the biotite zone, mica recrystallization be-

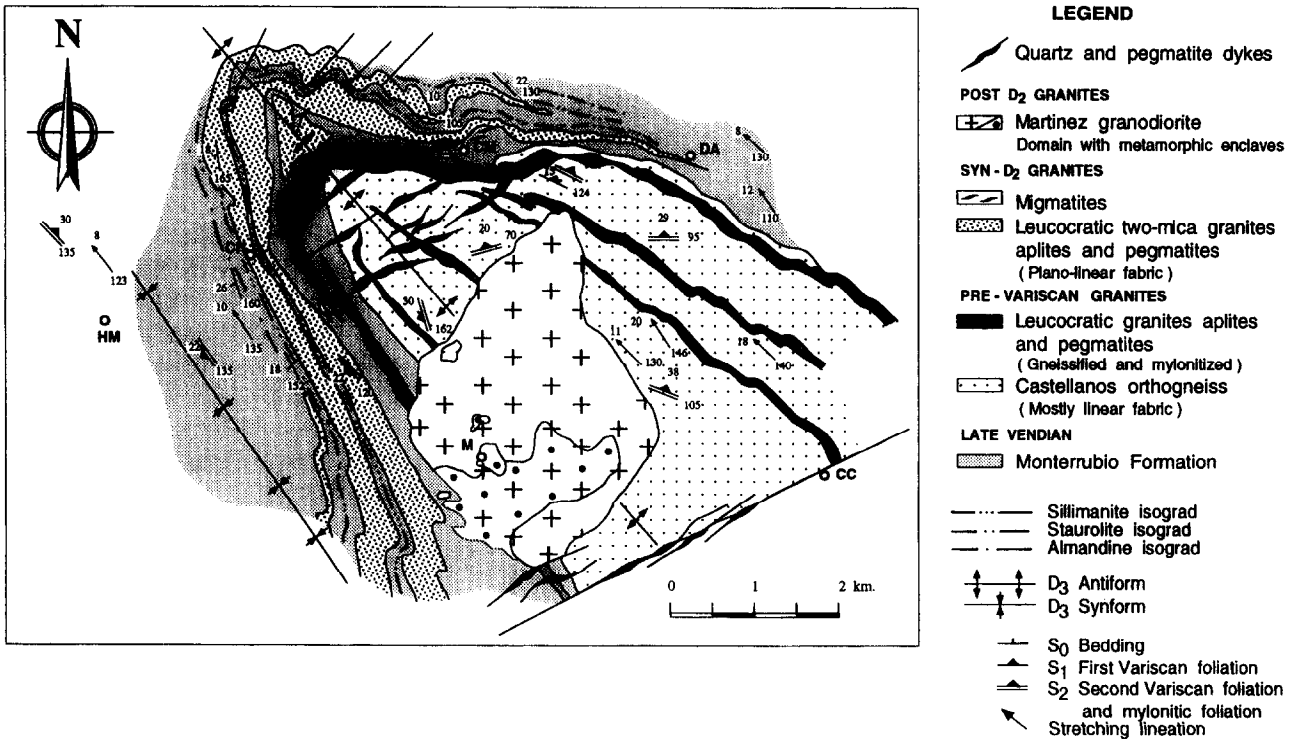

Fig. 4. Geological map of the Castellanos Antiform (see Fig. 2 for location). Localities: CH—Chagarcía Medianero. HM—Horcajo Medianero. CM—Carpio Medianero. DA—Diego Alvaro. M—Martínez. CC—Castellanos de la Cañada.

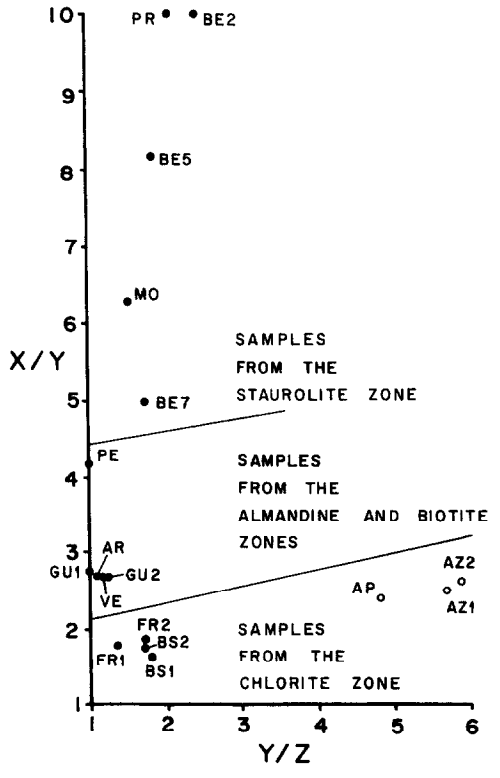

Fig. 5. Plot of the measured finite strain ellipsoids in a Flinn diagram. Open circles: dolomitic nodules in slates of the Aldeatejada Formation. Dots: quartzitic conglomerates of the Monterrubio Formation. The metamorphic zones where the samples were collected are indicated.

comes important, mostly towards the bottom. In general, D_2 strain is low in metapelites of these zones and no diagnostic criteria for rotational deformation have been found. The possibility that small normal faults contemporaneously affected the more competent Paleozoic sandstones and quartzites cannot be ruled out, but in any case, the brittle phenomena are clearly subordinate.

A steep strain gradient is observed around the almandine isograd, because the D_2 structures are quite different in the zones of almandine, staurolite and sillimanite. Minor D_2 folds are tight, often isoclinal (Figs. 10b & c), the interlimb angles ranging from 60° to 0°, with most values between 30° and 10° (Díez Balda 1986). Their hinges are sometimes curved, and sheath folds exist (Figs. 10d–f). The geometry of the folded competent layers is that of the class 1C close to class 2 (Ramsay 1967). The S_2 fabric, axial planar to the folds, is commonly a strong sub-horizontal tectonic foliation, which obliterates the S_1 cleavage. The most common fabric is a medium to coarse-grained schistosity in the pelitic and psammitic lithologies, locally banded in the former reflecting its crenulation origin. Foliation is also visible in the conglomerates, the quartzites and the orthogneisses, and often shows mylonitic characteristics in the latter two lithologies.

The abundance of minor folds, the strong sub-horizontal S_2 fabric with mylonitic characteristics, the presence of a commonly associated mineral and stretching lineation (also sub-horizontal and striking NW–SE), and the existence of kinematic indicators of rotational deformation in the zones of almandine, staurolite and sillimanite led Díez Balda (1983, 1986) to interpret these zones as forming part of a very wide sub-horizontal shear zone, presently outcropping in the core of a late antiform and in a tilted area to the SE (Fig. 9). The hangingwall of the shear zone would be the less-deformed chlorite and biotite zones, and the roof, the narrow band where the steep deformation gradient occurs. The following paragraphs deal with the strain within the shear zone, which is often referred to as the detachment, and the establishment of the sense of shearing from kinematic indicators.

Evaluation of D_2 *strain in the shear zone from the strain path.* As the only strain markers present in the area are in the metasediments, no independent estimation of the D_2 strain can be obtained, and only the finite $D_1 + D_2$ deformation can be measured. However, a possible approach to the problem is to assume that the D_2 deformation was superimposed upon D_1 strains characterized by ellipsoids of the type measured in areas of the chlorite zone, which were not affected by the second event. The only allowable markers are the quartzitic pebbles in conglomerates of the Monterrubio Formation, because they can be found both in the chlorite zone, above the detachment, and in the staurolite and sillimanite zones. The superimposed strain was probably heterogeneous, but the different ellipsoids measured could represent different values of superimposed strain and the analysis of several samples would give an idea of the strain path followed by the finite strain ellipsoid. Comparing this possible strain path with calculated paths corresponding to the superposition of different types of ellipsoids will give an idea of the kind and amount of superposed deformation undergone.

The R_f/Φ method was used for the finite strain analyses in the detachment zone, as in the case of the D_1 ellipsoid. The main difference is that, in this case, the fabric is dominantly linear in most cases. Consequently, the samples were cut normal to the stretching lineation, assumed to represent the X axis, the YZ plane was analyzed and, once the orientation of the axes Y and Z was obtained, the planes XY and XZ were cut and measured (Figs. 7b and 8b). Fry (1979) analyses were carried out in some of the samples, though this method is less precise in the case of the conglomerates due to the heterogeneities in pebble size. For the more deformed conglomerates, the ellipses are badly defined. However, the area without dots, where the ellipse can be inscribed, gives results similar to those calculated by the R_f/Φ method. This was expected because the matrix content is negligible.

Crystal plasticity processes seem the main mechanisms responsible for the deformation of the quartz pebbles. Though, in some samples, the pebble boundaries look somewhat serrated in close view, their shapes are ellipsoidal, and their surfaces are convex and rather regular, as can be seen quite often, when the rock is weathered and the pebbles become loose. No plane surfaces or noticeable interpenetration of some pebbles

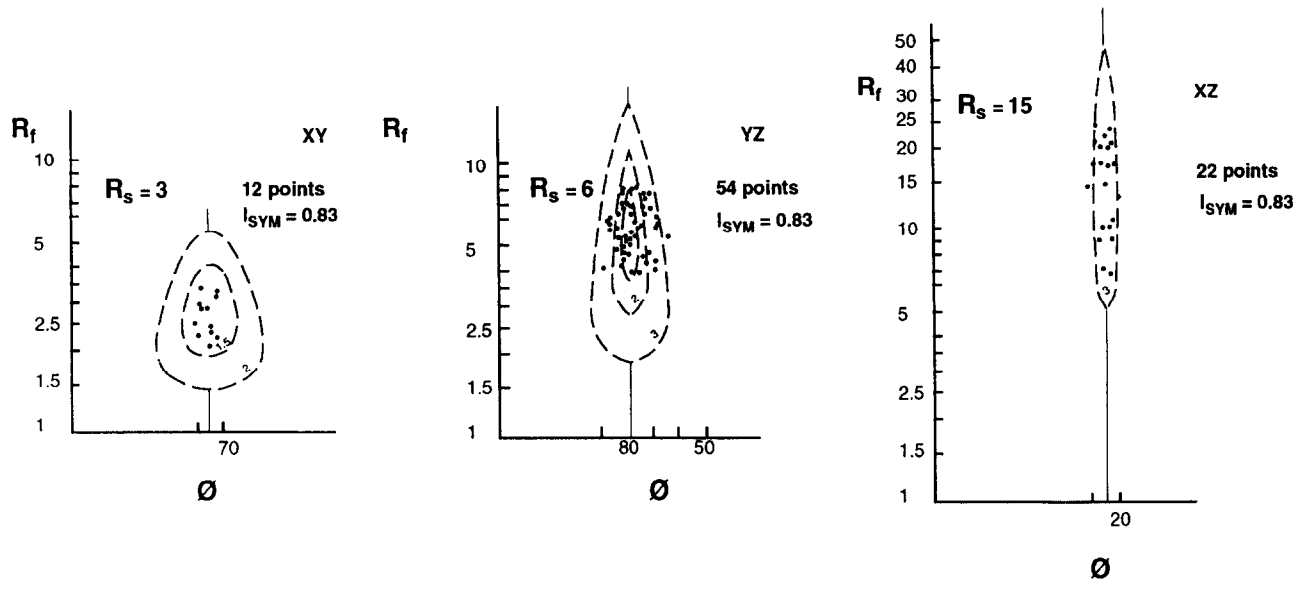

Fig. 6. R_f/Φ diagrams for dolomitic nodules in slates of the Aldeatejada Formation from Azud de Villagonzalo, sample AZ2. Principal planes *XY*, *YZ* and *XZ*.

by the adjacent ones are seen, suggesting that pressure-solution mechanisms, when they existed, were clearly subordinate. The crystallographic quartz fabrics in these rocks also point to an important component of crystal plasticity.

The strain results are plotted as dots in Fig. 5, with indication of the metamorphic zones where they were collected. Several samples lie close to the vertical axis (prolate ellipsoids) with values of X/Y between 2.7 and 4.1, and several others, more deformed, are in the field of apparent constriction, with values of X/Y between 5 and 10 and Y/Z between 1.7 and 2.4. In all of them, the X axis is sub-horizontal, striking roughly NW–SE and, when it exists, the XY plane is sub-horizontal, the small departures from these orientations being attributable to the late open folds.

In order to calculate the theoretical strain paths, it was assumed that the initial ellipsoid was that shown by similar rocks outside the D_2 shear zone. The superposition was calculated separately assuming pure shear and simple shear, by the method described by Ramsay (1967, pp. 81–94), involving the use of the strain invariants, and is fully described in Díez Balda (1983).

Some reasonable assumptions regarding the orientation of the axes were made. For the case of pure shear, coaxiality between the axes of the first and second ellipsoids was assumed, the X axis being coincident for both ellipsoids, in keeping with the fact that the X axis of the finite $D_1 + D_2$ ellipsoids in the shear zone is always parallel to the measured X axis of the D_1 ellipsoids outside the shear zone and also because biotites syn-kinematic to D_2 define a mineral lineation roughly NW–SE and horizontal. The Y and Z axes were interchanged, given the fact that D_1 gave rise to a vertical cleavage (Z axis horizontal) and D_2 to a horizontal foliation (Z axis vertical). For non-coaxial deformation, simple shear *sensu stricto* was assumed, with the shear plane horizontal, i.e. parallel to the XZ plane of the D_1 ellipsoid, and the shear direction parallel to the X axis of D_1. These assumptions are justified by the data collected from kinematic indicators, as described below.

For the case of pure shear, several strain paths were calculated for constant k values of 0, 0.2, 0.4, 0.6, 0.8, 1 and 2, and for two different starting ellipsoids (FR1 and BS1, Figs. 11a & b respectively), applying superimposed ellipsoids with increasing values of X/Z. For simple shear ($k = 1$), a strain path was obtained for each of the same two starting ellipsoids. The strain paths for simple shear are identical to those of pure shear with $k = 1$. The paths are depicted as thin lines in Fig. 11, together with the strain measurements in the conglomerates. The numbers along them are the X/Z values for coaxial deformation, and the framed numbers along the $k = 1$ path represent the γ values of the superimposed simple shear. As can be seen, the strain paths are open curves coming out from the starting ellipsoids and reaching the vertical axis, which means that all of them pass through the prolate type ellipsoids. From the vertical axis onwards, they continue as straight lines with a slope varying from horizontal, for $k = 0$, to very steep for k values close to 1 and higher.

A regression line (dashed in Figs. 11a & b) was calculated for the more deformed samples (BE2, BE5, BE7, MO, PE and PR). It could represent stages of the strain superposition and, from the prolate finite ellipsoid onwards, it may be compared to the theoretical paths obtained. The line is very close to the straight part of the $k = 1$ strain path, which suggests that the assumptions are reasonable and that, inside the shear zone, the D_1 ellipsoids were progressively transformed into truly prolate ellipsoids and then followed a straight strain path in the field of apparent constriction.

The samples from the chlorite zone underwent very little or no D_2 deformation; the samples close to the vertical axis, with a X/Y ratio around 3, come from the zone of biotite and from the narrow almandine zone,

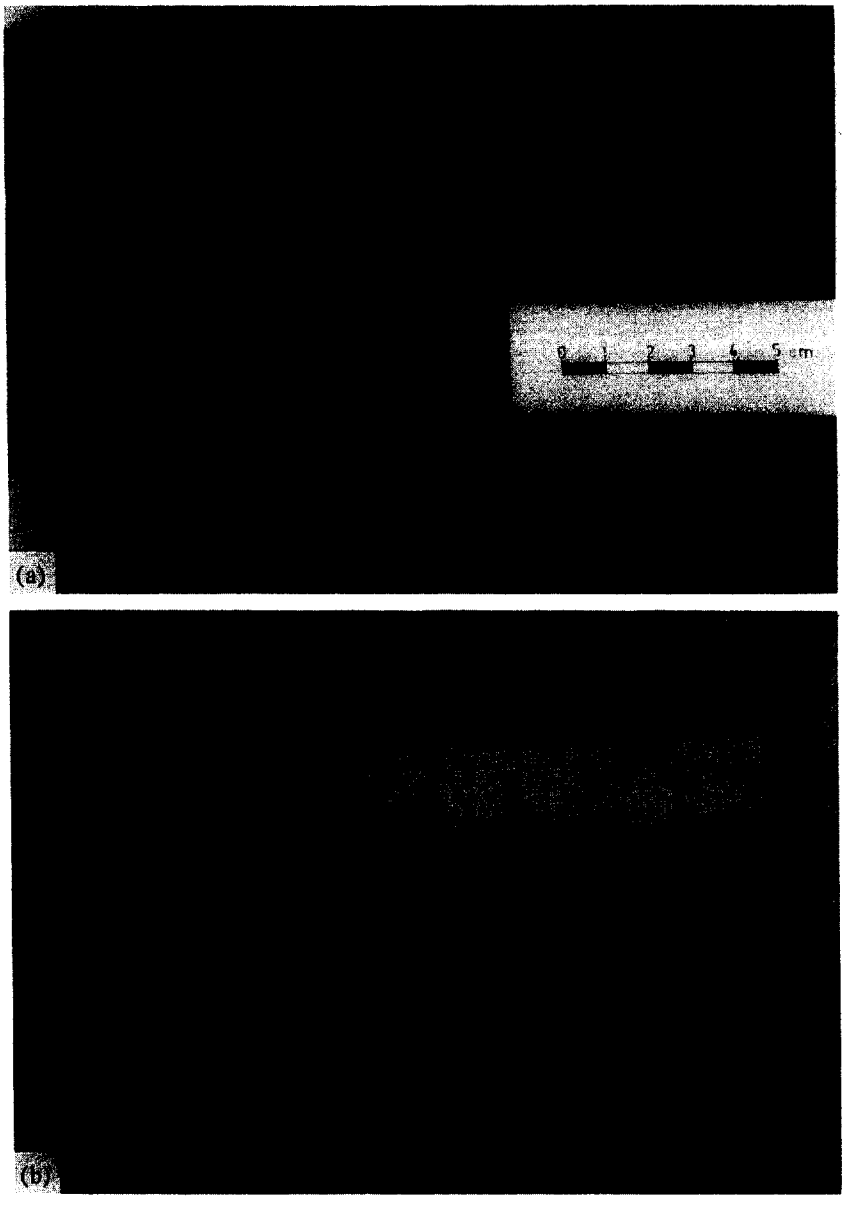

Fig. 7. (a) Aspect of the dolomitic nodules of Azud de Villagonzalo, sample AZ1. The planes are *XZ* (above) and *XY* (below). (b) Deformed conglomerate of the Monterrubio Formation in Beleña, sample BE5, plane *XY*.

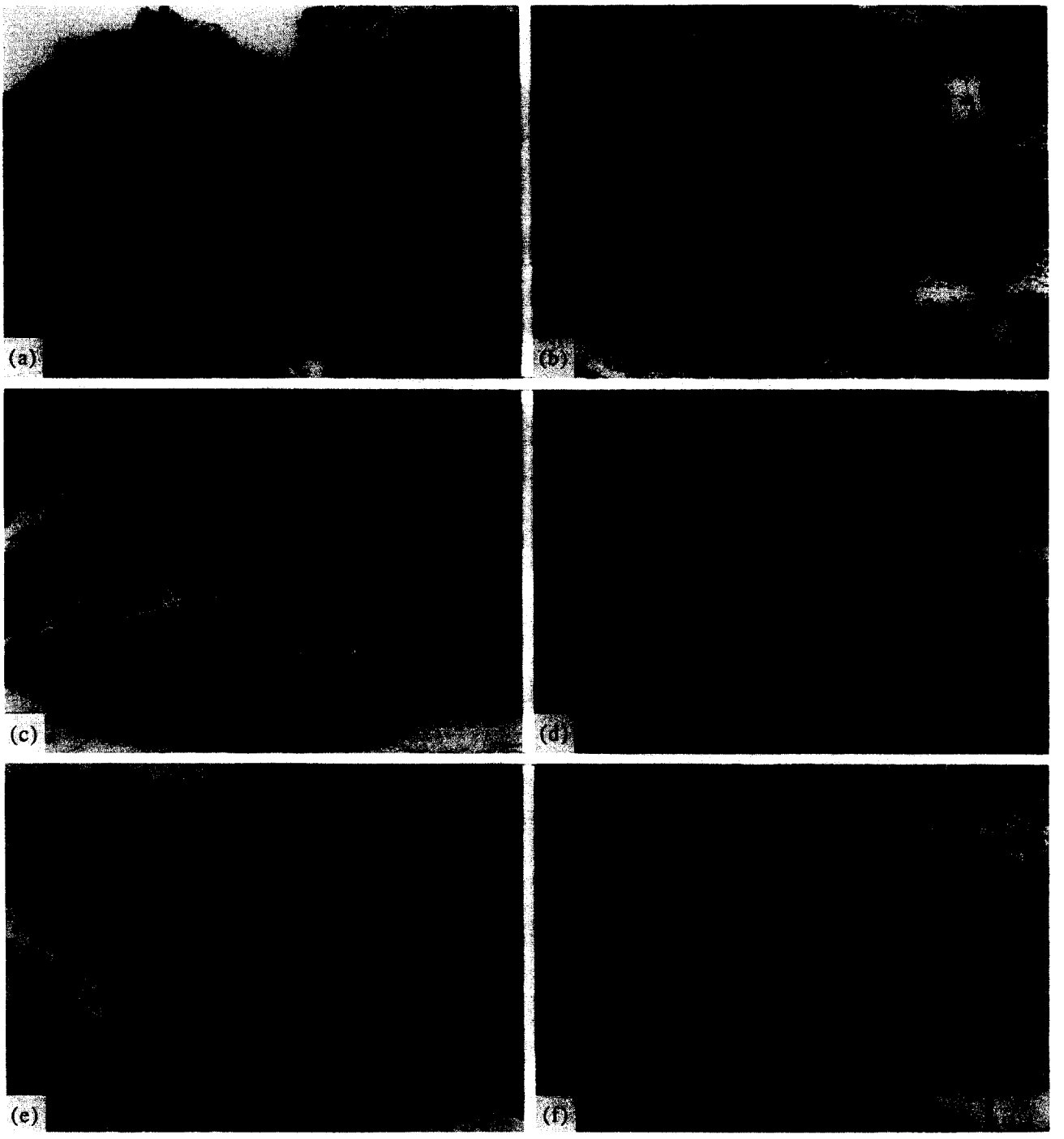

Fig. 10. Different aspects of D_2 folds. (a) Open folds in Azud de Villagonzalo, in the chlorite zone, hangingwall to the detachment zone. (b) Tight folds in the staurolite zone close to Alba de Tormes. (c) Isoclinal folds in the sillimanite zone southeast of Guijo. (d), (e) & (f) Sheath folds shown in section normal to the shear direction in the sillimanite zone, southeast of Guijo.

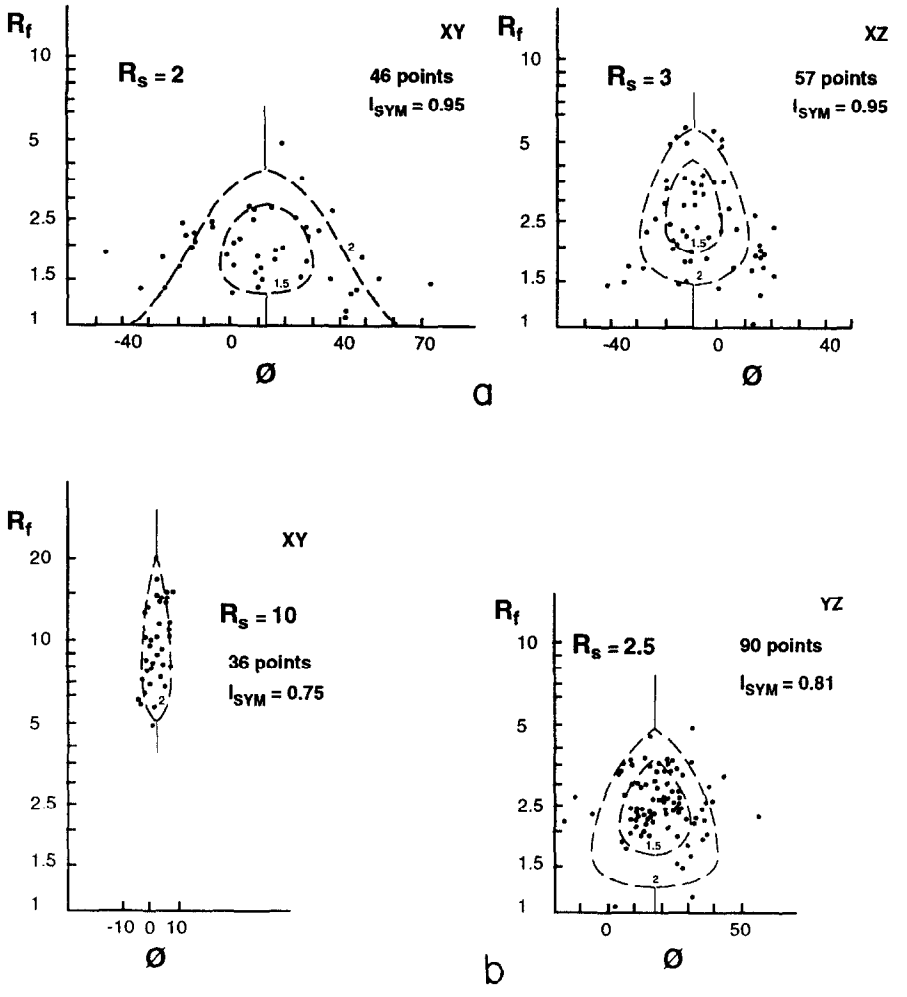

Fig. 8. R_f/Φ diagrams from quartzitic conglomerates of the Monterrubio Formation. (a) Sample FR1, from Frades, in the chlorite zone. Principal planes XY and XZ. (b) Sample BE2, from Beleña, in the staurolite zone. Principal planes XY and YZ.

and represent ellipsoids with weak D_2 superposition, and the more deformed samples, from the staurolite zone, underwent strong D_2 deformation in the shear zone. The inset in Fig. 11(b) depicts the progressive changes undergone by the finite strain ellipsoid through D_2. Although they do not prove it, these results agree with the assumption that the essential deformation mechanism was simple shear, as the D_2 ellipsoid seems close to the plane strain type. The higher measured strains would, in this case, represent a shear strain (γ) around 3.5 for the superimposed D_2 ellipsoid.

Deformation of the granitic rocks

The granitic rocks outcropping in the meso and catazonal areas were variably deformed, and it is possible to differentiate two groups according to their deformation characteristics. The first group includes biotitic granitoids that were intruded by leucocratic granites, aplites and pegmatites and, subsequently, tectonized and often mylonitized. The biotitic orthogneisses of San Pelayo, in the Martinamor Antiform, and those of Castellanos and Bercimuelle, in the southeast of the area (Figs. 2 and 4), belong to this group. The Variscan or pre-Variscan age of these granites has been discussed and some radiometrical dating has been carried out in San Pelayo. Linares *et al.* (1987) reported a Rb–Sr whole rock age of 430 Ma, whereas Galibert (1984) obtained an age of 332 ± 13 Ma by the U–Pb method in zircons (lower intercept of a discordia, the upper intercept being 1893 ± 9 Ma), but a monazite population gave an age of 351 ± 9 Ma.

The fabric in the rocks of the first group is planolinear to linear ($L > S$), often mylonitic, being predominantly linear in the Castellanos Orthogneiss. The stretching lineation is sub-horizontal, striking NW–SE in all of the massifs, and the foliation plane, when visible, is weakly dipping and parallel to S_2 in the adjacent metasediments. The type of fabric and the orientation of the planar and linear elements on the orthogneisses is similar to that of the conglomerates described above. Also, a relic foliation, normal to the main sub-horizontal schistosity, is commonly seen in thin section in the Castellanos Orthogneiss and can also be observed in the outcrop. For these reasons, it is deduced that they underwent the same deformation events as the country rocks and, consequently, that they are clearly pre-Variscan. The U–Pb Variscan ages (Galibert 1984) probably reflect the metamorphism, because the orthogneisses are in the sillimanite zone.

The second group is made up of the leucocratic two-

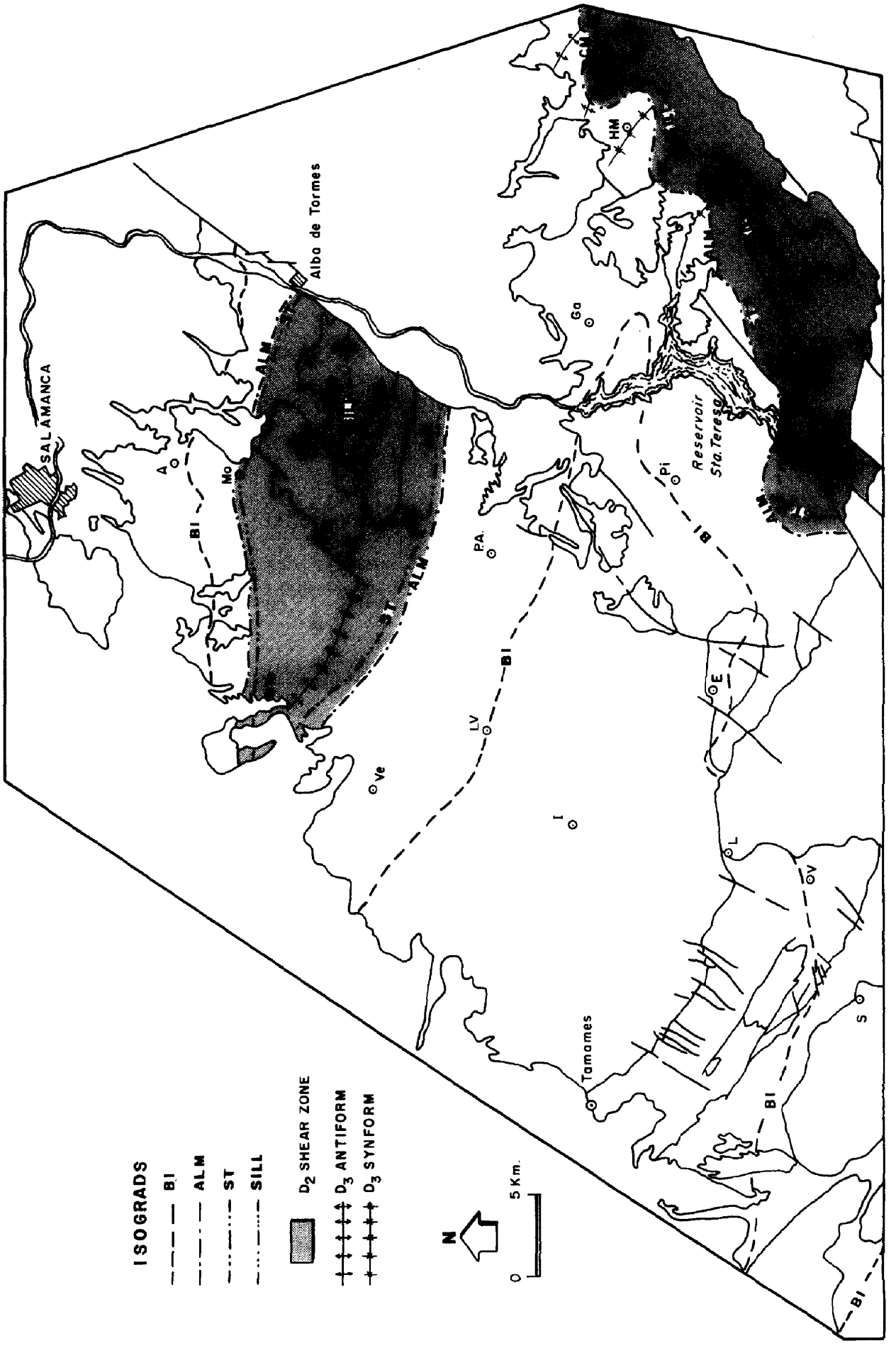
ISOGRADS
BI
ALM
ST
SILL
D2 SHEAR ZONE
D3 ANTIFORM
D3 SYNFORM
N
0
5 Km.
SALAMANCA
Alba de Tormes
Reservoir
Sta. Teresa
Tamames
A
Mo
PA.
Ve
LV
I
Ga
HM
Pi
E
L
V
S

Fig. 9.

mica granites, aplites and pegmatites of Martinamor, Cespedosa, Carpio Medianero and others. They are lenticular bodies, parallel to S_2 in the country rock and often boudinaged. The internal deformation is variable but always less than in the granitoids of the first group. The fabric is plano-linear ($L \approx S$), never dominantly linear, with the foliation plane sub-horizontal and the stretching lineation striking NW–SE and sub-horizontal.

The heterogeneous character of the deformation is depicted by the different intensities of the fabric and by the presence, in some bands or bodies, of *S–C* structures, but all the fabrics are attributable to D_2 (and, locally, to narrow D_3 shear zones), and no previous fabric has been identified. As the strain ellipsoid of the second phase seems to be of the plane strain type, the one that would typically produce a plano-linear fabric, these rocks are considered syn-kinematic to D_2. They were generated by partial melting of underlying rocks, probably the orthogneisses of the first group, because evidence of incipient migmatization can be seen in them. Migmatitic veins in the leucocratic orthogneisses often appear boudinaged, and folds similar to those of D_2 in the country rocks affect the veins and aplitic dikes.

The granitoids of the second group were probably intruded along dilational openings that could have been sub-horizontal in origin, as was proposed for a similar situation by Holcombe *et al.* (1991).

Kinematic criteria

Two aspects are important regarding the kinematics of the D_2 deformation, the shear direction and the shear sense. In shear zones with high shear strains, the long axis of the finite strain ellipsoid gives a good approximation to the shearing direction. In our case, the mineral lineation, visible in many rocks of the shear zone, and the stretching lineation in the quartzitic conglomerates are thought to represent the X axis of D_2 strain. Consequently, a sub-horizontal NW–SE shearing direction is suggested. However, as D_2 overprints a previous deformation, we have preferred to obtain an independent estimate of the shearing direction by two different methods.

The first is the analysis of D_1 lineations folded by D_2 (Ramsay 1967). The flow direction obtained in minor folds varies between 124° and 136° (Fig. 12). The second is the separation angle method (Hansen 1971), based on the apparent change in asymmetry from one side to the other of the flow direction in folds with curved hinges and in populations of folds with highly dispersed hinges, due to the reorientations undergone in ductile shear zones. The hinge orientations and apparent asymmetries of minor folds were measured in an outcrop southeast of Guijo, in the Tormes River, which also depicts D_2 mesoscopic folds (Fig. 13a). The mesoscale folds are recumbent (Fig. 13b) and the two stereoplots show the hinge lines and asymmetries of D_2 minor folds in the steeply-dipping limbs (Fig. 13c) and in the less-dipping limbs (Fig. 13d) of the mesoscale folds. The flow directions obtained, well-defined by narrow separation angles, are 136° and 127°, respectively.

For finding the shear sense, the most reliable criteria in the area are the *S–C* structures (Berthé *et al.* 1979) and the porphyroclast microstructures (Passchier & Simpson 1986). *S–C* structures of type I (Lister & Snoke 1984) exist in deformed syn-kinematic granites, and are particularly well developed in a lenticular body south of Cespedosa. Type II *S–C* mylonites are common in the Castellanos and San Pelayo orthogneisses. Both types indicate a consistent top to the SE shear sense. Porphyroclast systems of σ type around feldspars in the orthogneisses also indicate the same sense of shear.

Quartz *c*-axis fabrics were investigated in 20 oriented mylonite samples distributed along the Martinamor and Castellanos Antiforms, inside the shear zone. The samples come from intensely stretched quartzitic conglomerates and from mylonitic orthogneisses with more than 30% quartz. Figure 14 shows some of the quartz diagrams from mylonites, which correspond to two of the types described by Schmid & Casey (1986).

Single *c*-axis girdles: samples PAS-79 and PAS-89 are essentially of this type, though they depict small submaxima deviated from the main girdle and the latter is transitional to the type I crossed girdles. This pattern is indicative of simple shear deformation (Burg & Laurent 1978, Bouchez *et al.* 1979) with slip in the <*a*> direction, the girdle being a result of the preferred alignment of the *a*-axes into parallelism with the bulk shear direction. These diagrams cannot be reliably used to infer the sense of shear, because they are practically orthogonal to the foliation. However, they are indicative of high shear strains.

Type I crossed girdles: samples PAS-92 and PAS-83 can be considered roughly of this type, which is characterized by the tendency of two *c*-axis girdles to meet at some distance from the intermediate strain axis and to be connected with the symmetric counterpart via a single girdle more or less orthogonal to the foliation. In sample PAS-83, the central single girdle is incomplete and in PAS-92, it is oriented roughly orthogonal to the foliation. Consequently, the shear sense cannot be established. However, this kind of pattern suggests, according to Schmid & Casey (1986), that coaxial components were involved in the deformation, which was roughly of plane strain type in any case.

The third deformation phase (D_3)

Open folds with wavelengths up to 12 km are characteristic of the third phase. Their axial surface is sub-

Fig. 9. Map showing the distribution of metamorphic isograds in pelites and the D_2 shear zone (grey). BI—Biotite. ALM—Almandine. ST—Staurolite. SILL—Sillimanite. Note the parallelism between the upper limit of the shear zone and the almandine isograd. Localities: A—Arapiles. Ar—Armenteros. B—Beleña. C—Cespedosa. CM—Carpio Medianero. E—Endrinal. G—Guijuelo. Ga—Galinduste. GA—Guijo de Avila. HM—Horcajo Medianero. I—Iñigo. L—Linares. LV—Las Veguillas. M—Morille. Ma—Martinamor. Mo—Mozárbez. MS—Monterrubio de la Sierra. Pa—Pedrosillo de los Aires. Pi—Pizarral. R—Revilla. S—Sequeros. To—Tordelalosa. V—Valero. Ve—Vecinos.

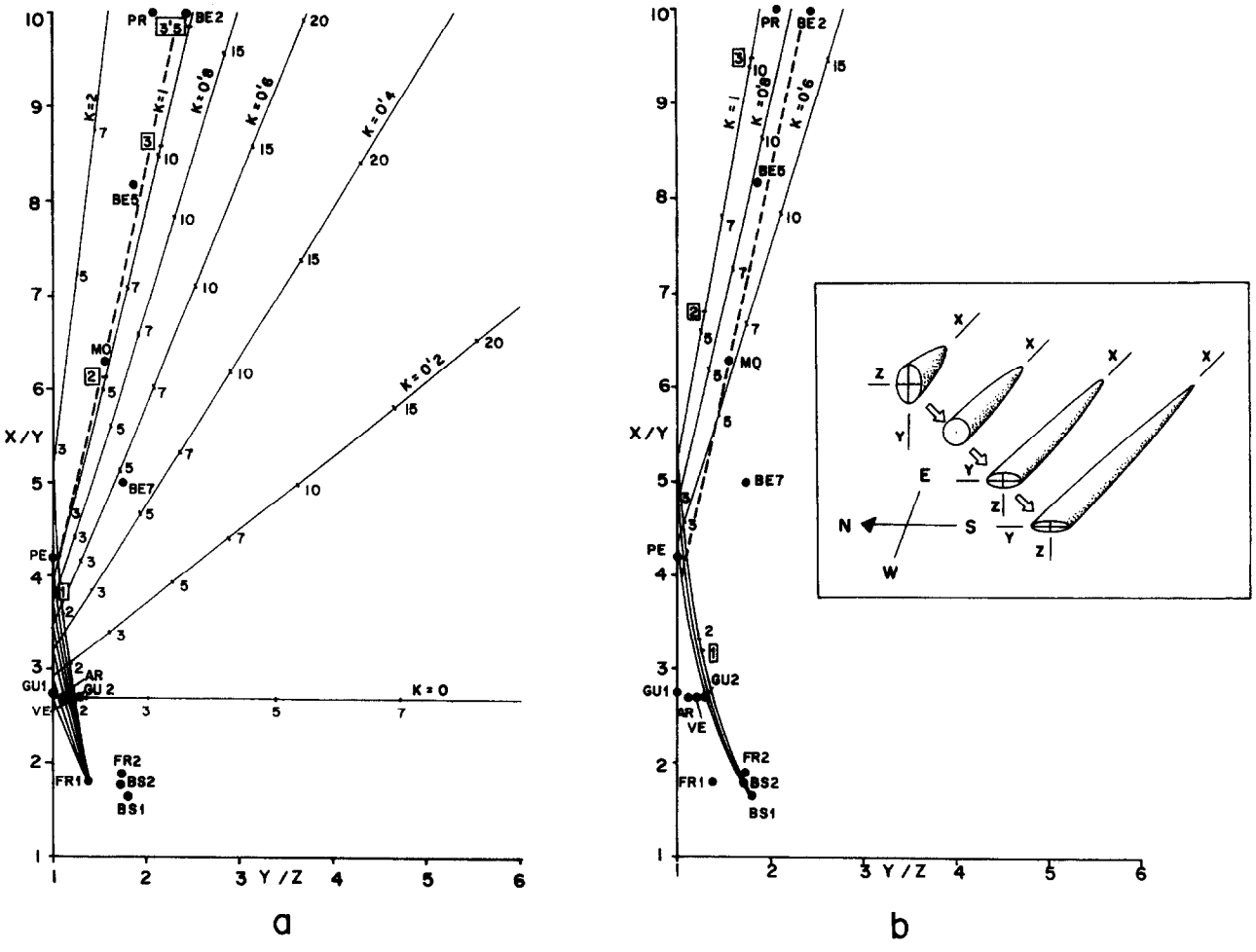

Fig. 11. Flinn diagram for the quartzitic conglomerates of the Monterrubio Formation and calculated strain paths assuming pure and simple shear (see text for details). Thin lines represent strain paths for the indicated k values of the superimposed ellipsoid. Numbers along them are the values of X/Z of the superimposed ellipsoid and the framed numbers along the $k = 1$ path are the values of shear strain for the case of simple shear. The dashed line is a regression line for the measured ellipsoids of prolate and constrictional types, in order to compare with the calculated strain paths. (a) & (b) show strain paths calculated from two different ellipsoids measured outside the shear zone: samples FR1 and BS1. Inset in (b) shows schematically the evolution of the finite strain ellipsoid through the D_2 event. The initial D_1 ellipsoid is the one in the upper left corner.

vertical, striking 110°–120° and often, they show an axial planar crenulation or a poor crenulation cleavage. The associated strain is very weak, so that its effects on the fabric of the rocks can be considered negligible. These structures fold the metamorphic isograds and the ductile shear zone, as can be seen in the core of the largest of these folds, the Martinamor Antiform, and also in the southeast of the studied area, where several D_3 folds are also mappable (Figs. 2, 4 and 9). Minor sub-vertical shear zones with strike-slip movement are common, specially in the granitoids.

THE METAMORPHISM AND ITS RELATIONSHIP TO THE DEFORMATION

The textural relationships in the pelitic rocks show a prograde continuous evolution, from D_1 to the first stages of D_2, involving the growth of chlorite, biotite, almandine, staurolite and probably sillimanite. This implies a sequence of the intermediate pressure type, evidenced by the stability of the garnet–staurolite pair. Even if kyanite has not been identified, this event is loosely referred to as Barrovian, and was supposedly contemporaneous with the crustal thickening. The biotite, garnet and staurolite show inclusions depicting an internal foliation, S_i, somewhat curved, which is interpreted as the S_1 slightly bent by D_2. However, the S_2 outside the porphyroblasts is very flattened and always develops pressure shadows around them, suggesting a previous or early growth of these index minerals with respect to D_2.

The subsequent evolution shows a transition to a low-pressure type of metamorphism during D_2, which culminated in the growth of andalusite and cordierite porphyroblasts, late-kinematic in relation to S_2. Often, the earlier garnet, staurolite and sillimanite appear as small relics, the staurolite being transformed into andalusite and biotite and the cordierite growing in the rims of staurolite and including fibrolite crystals. The change to lower pressure conditions occurred under conditions of stability of sillimanite in the sillimanite zone, because fibrolite is commonly parallel to S_2, suggesting a syn-kinematic growth.

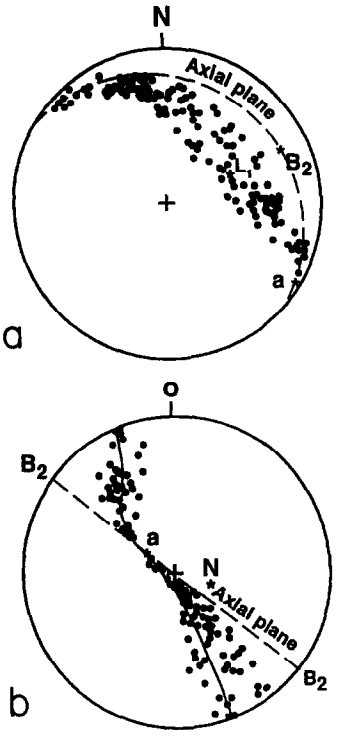

Fig. 12. D_1 intersection lineation between bedding and S_1, deformed by a D_2 fold in Morille, in the core of the Martinamor Antiform. (a) Locus of the folded lineation in its actual orientation. The axial plane and fold axis (B_2) is given as reference. (b) Same as previous but rotated, with the axial plane vertical and the axis horizontal, for comparison with the patterns deduced by Ramsay (1967, chapter 8). The slip or flow direction, *a*, is obtained from the intersection between the lineation locus and the axial plane. This is then rotated back to the original position in the above diagram.

The metamorphic conditions for the first stage can be deduced from the stable pair garnet and staurolite, indicative of an intermediate pressure gradient. *PT* conditions of around 4 or more kbar and 600–700°C can be assumed in the sillimanite zone. The second metamorphic stage depicts a decrease in pressure of more than 2 kbar at the end of D_2, indicated by the stability of andalusite (Fig. 15), whilst the temperature remained elevated during the whole deformation, as indicated by the migmatization in the lower levels, the secondary character of the muscovites in the migmatites, and the thorough recrystallization undergone by all the rocks in the shear zone.

Finally, a third, retrometamorphic stage can be identified by the transformations of biotite to white mica and chlorite and of the index minerals to aggregates of micaceous products. From textural relationships, these changes are essentially post-kinematic in relation to D_2 and indicative of a decrease in *T* in the presence of fluids. S_3 crenulation cleavages were developed, and also late ductile shear zones with greenschist facies assemblages.

DISCUSSION

The microstructures and the inferred strain indicate that the main D_2 structure in the area is a sub-horizontal shear zone, several km thick. Criteria indicative of simple shear include the development of *S–C* structures of both types I and II (Lister & Snoke 1984), the existence of porphyroclast systems of σ-type around feldspars and the presence of single *c*-axis girdles among the quartz crystallographic fabrics. The probable D_2 strain ellipsoid, calculated from the strain paths in conglomerates, and the type I crossed girdles in quartz fabrics, suggest a plane strain type of deformation, which accords with a simple shear mechanism. However, the possibility that coaxial components were also involved in the deformation cannot be ruled out and, in fact, are suggested by the above-mentioned type I crossed girdles.

Furthermore, there is a strong D_2 deformation gradient in the upper limit of the almandine zone and no important rotational deformation took place in the biotite and chlorite zones. This implies that two differently deformed rock units are mutually in contact without any fault or other kind of discontinuity between them. Considering the strain compatibility between both units, the logical conclusion is that the unit strongly deformed by D_2 is in fact a shear zone whose upper limit crops out in the study area, but whose lower limit does not. The uncertainty concerning the existence of the lower limit, together with the possible presence of coaxial components in the deformation, suggests that it should be considered as a *sensu lato* shear zone and the deformation mechanism as general simple shear (Simpson & De Paor 1993).

The deformation in the shear zone is heterogeneous, but generally strong, involving the mylonitization of pre-Variscan granitoids, and developing an intense stretching lineation in quartzitic conglomerates of the Monterrubio Formation. Kinematic criteria are consistent with displacement of the rock unit above the shear zone towards the southeast, the zone itself acting as a broad detachment zone and the epizonal rocks being its hangingwall unit.

The strain gradient coincides spatially with a strong metamorphic gradient: there is a rapid transition from slates of the biotite zone to highly crystalline schists with almandine and staurolite. In some areas, such as north of Martinamor (Fig. 9), the transition occurs over a few dozen meters. There is a thinning of the Barrovian metamorphic zones and the virtual disappearance of some of them, namely that of almandine and, locally, also that of staurolite (Fig. 9), indicating that a part of the metamorphic pile is missing. This implies that we are dealing with an extensional shear zone and, according to the sense of movement deduced, it should have been originally inclined to the SE (Fig. 16a). This dip is also suggested by the distribution of the Barrovian isograds: the staurolite zone is broad in the Martinamor Antiform, to the north of the area, but disappears in the Castellanos Antiform, to the southeast (Fig. 9). This points to a deepening of the top of the shear zone to the southeast.

The complete geometry of the extensional detachment zone has not been established because its dimension exceeds that of the area studied and also because it

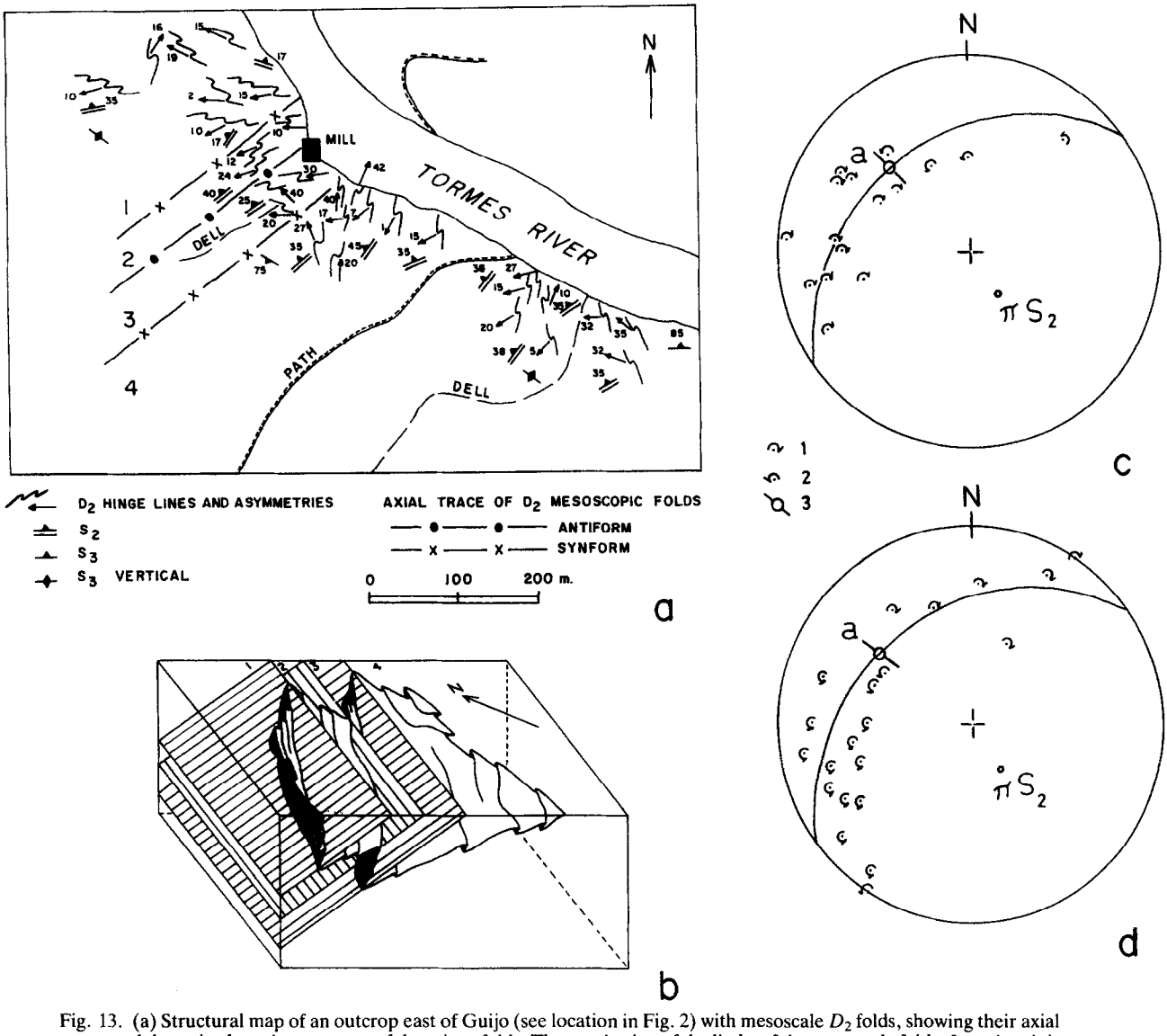

Fig. 13. (a) Structural map of an outcrop east of Guijo (see location in Fig. 2) with mesoscale D_2 folds, showing their axial traces and the attitude and asymmetry of the minor folds. The numbering of the limbs of the mesoscale folds, from 1 to 4, is used as reference for the block diagram in (b). (c) & (d) Plot of the hinge lines and asymmetry of D_2 minor folds of the outcrop mapped in (a) to obtain the flow direction (Hansen 1971). (c) limbs 1 and 3, (d) limbs 2 and 4, (1) clockwise asymmetry, (2) anticlockwise asymmetry, (3) deduced flow direction.

is cut to the southeast by a huge batholith. To the northwest, it can be followed until it is cross-cut by the Juzbado-Penalba do Castelo shear zone, which runs with a direction 70° and outcrops 20 km to the northwest of the town of Salamanca. This is a narrow sinistral ductile fault, with a horizontal displacement estimated between 65 and 100 km (Iglesias Ponce de León & Ribeiro 1981, Villar Alonso *et al.* 1992). North of this structure, a similar extensional detachment has been identified in the so-called Tormes Gneiss Dome (Escuder Viruete *et al.* in press), with the same characteristics and the same sense of movement. It is worth noting that in the Tormes Gneiss Dome, the upper and lower boundaries of the detachment crop out, so that its description as a general shear zone is admissible. Both detachments are probably part of an important family of extensional structures developed subsequently to the D_1 compressional event but deformed by the late D_3 folds and wrench shear zones. As both D_1 and D_3 resulted from the Variscan collision, the extensional event is considered syn-collisional and produced by the gravitational collapse of the orogen. A relationship of D_2 with gravity instabilities had been suggested by Noronha *et al.* (1981).

Once the average topographic elevation induced by the convergence reached a threshold [of between 3 and 5 km according to Dewey (1988) and Block & Royden (1990)], the collapse probably initiated in the mid-crustal levels as a broad zone of deformation including the almandine, staurolite and at least part of the sillimanite zones. Some index minerals indicative of Barrovian metamorphism did grow in the first stages of D_2, reflecting the fact that the lithostatic pressure was still high, but later on the mineral parageneses reflect a decompression under conditions of maintained high temperature, indicated by the syn-D_2 sillimanite and by the injection of migmatitic veins and the intrusion of leucocratic two-mica granites, aplites and pegmatites. The late-D_2

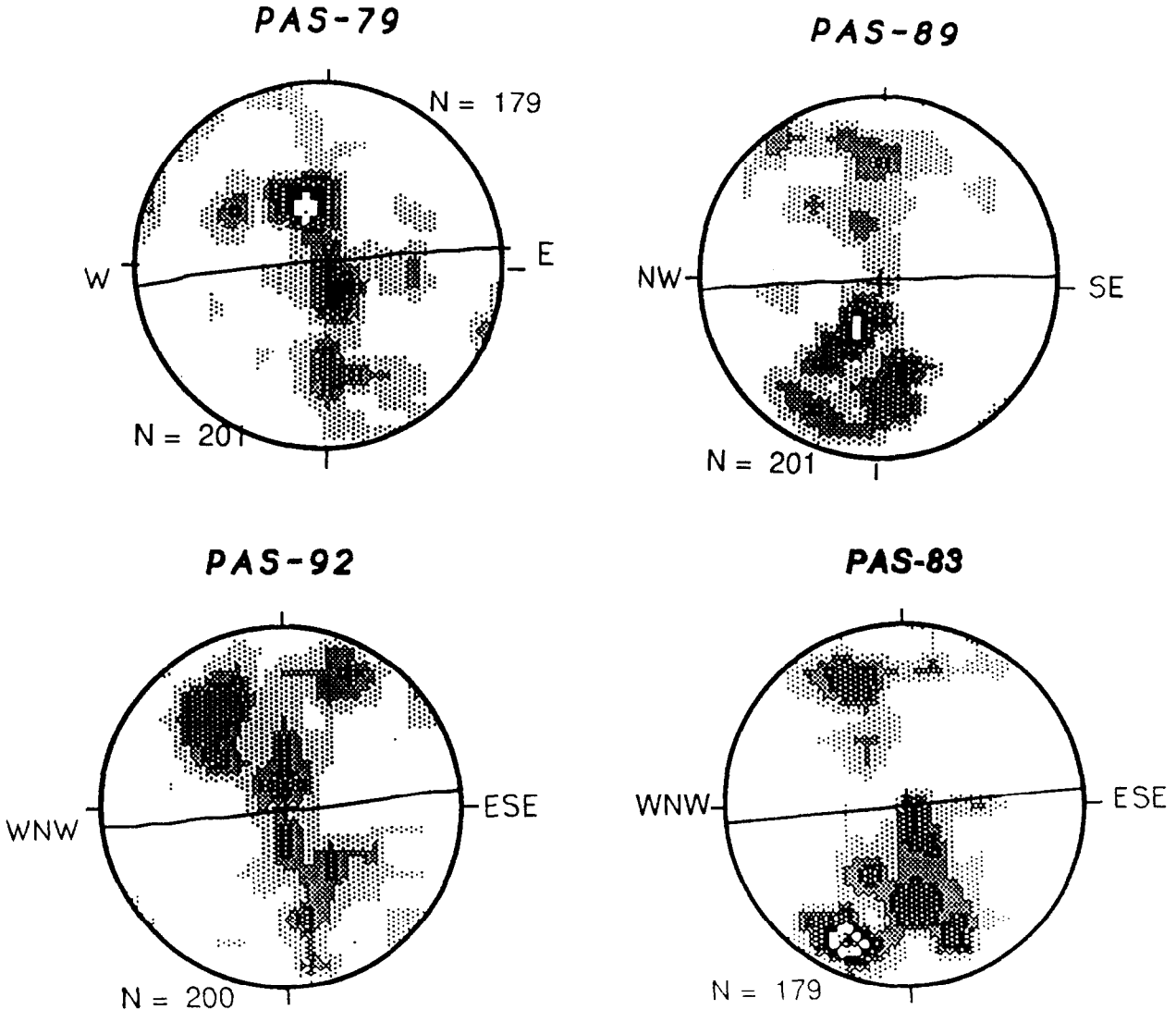

Fig. 14. Quartz *c*-axis fabrics from quartzitic mylonites in the Castellanos Antiform. The great circles represent the S_2 foliation, sub-horizontal in the field, and the poles of the stretching lineation are in their extremes. The fabrics suggest plane strain and simple shear components.

growth of andalusite and cordierite points to a decrease in pressure of more than 2 kbar during the extensional event (Fig. 15).

A comparison with metamorphic core complexes is difficult, because the continuation of the detachment zone into upper crustal levels is not seen in the area. The brittle character of the upper limit of the detachment zone, so common in the metamorphic core complexes (Lister & Davis 1989), is not observed here. On the contrary, some ductile deformation occurred in the low-grade hangingwall unit: a sub-horizontal crenulation of relatively low intensity developed, apparently not associated with rotational components (Fig. 16a). The reason that may account for the differences with the core complex model is that the extension in the present case was not enough to place the cold upper plate on top of the metamorphic rocks, and the hangingwall maintained the greenschist facies conditions during most of the extensional process.

Two main peculiarities of the gravitational collapse in the south of Salamanca are that the extension occurred in a direction parallel to the trend of the belt and that it took place in an area where the previous structures were folds with vertical axial surfaces (Fig. 16b). The first character has been described also in other orogens, such as the Himalayas, the Alps, the Carpathians and the Andes (Dewey 1988), and seems to be characteristic of syn-collisional collapse, as the continued convergence inhibits extension at high angle to the orogenic trend (Gapais *et al.* 1992).

The second feature is more unusual and deserves more attention. It is commonly admitted that crustal thickening able to trigger the gravitational collapse is caused by the stacking of nappes bounded either by brittle thrusts or by ductile compressional shear zones, the latter case commonly being equivalent to recumbent fold nappes (Hatcher & Hooper 1992). This implies translations of crustal slices in a direction which is roughly parallel to the Earth's surface and is usually described in the French literature as tangential tectonics.

The area south of Salamanca is characterized by a type of compressional tectonics that can be described as steep, because the main structures are folds with vertical

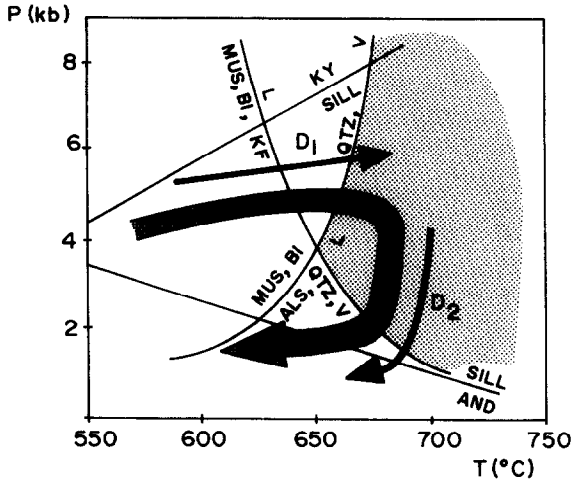

Fig. 15. *PT* path followed by the rocks of the sillimanite zone during the D_1 and D_2 deformations, showing a decrease in pressure of more than 2 kbar during the second event. The nearly isothermal path during D_2 is postulated according to the extensional character of this event, deduced from the lack of part of the metamorphic zonation. Partial petrogenetic grid based on Vielzeuf & Holloway (1988). Phase diagram for Al_2SiO_5 polymorphs after Powell & Holland (1988). Grey area represents conditions where partial melting may develop and muscovite is unstable.

axial surfaces and a generalized sub-vertical cleavage. This occurs not only here, but in a zone more than 200 km wide, the Domain of Vertical Folds of the CIZ (Fig. 1), and is not the consequence of refolding of previous recumbent structures.

It may be a case of a listric attitude of the cleavage, sub-vertical in the upper crustal levels but becoming progressively sub-horizontal at depth, as it merges with a deep décollement (Matte 1988). If this is the case, the change in inclination of the cleavage should occur at depths greater than the deepest levels outcropping here, because well inside of the detachment zone, the geometry of D_1 major folds can be seen, and their axial surface is still vertical (as in the southeast area, between Cespedosa and Armenteros, Fig. 2). Note that even if the parts of the major D_1 folds affected by the shear zone are strongly deformed, their profile in a cross-section vertical and normal to both their axis and the shear direction should be identical to the initial profile, providing that the folds were perfectly cylindrical, the D_2 deformation mechanism was perfect simple shear and the shear direction was parallel to the D_1 fold axes (Fig. 16a). In addition, the dominantly constrictional finite strain ellipsoids measured in the conglomerates of the detachment zone are well explained by the superposition of two deformations, the first having a sub-vertical XY plane. This strongly contrasts with the adjacent Domain of Recumbent Folds of the CIZ and the nearest West Asturian-Leonese Zone, where the recumbent folds affect the whole Proterozoic and Paleozoic sequences up to the Lower Devonian (Matte 1968, Díez Balda *et al.* 1990, Martínez Catalán *et al.* 1992).

It is quite evident that the steep tectonics was able to induce a crustal thickening sufficient to develop a prograde metamorphism of the intermediate pressure type, up to the sillimanite zone. As mentioned in the description of the first deformation phase, the thickening was probably achieved by a combination of pure shear and transcurrent simple shear, and a mechanism of sinistral transpression has been proposed by Dias & Ribeiro (1991a,b). The question is whether this mechanism was enough to induce the gravitational collapse.

It is impossible to get an unequivocal answer without more complete knowledge of the structure of the crust in the area, but some insights can be obtained from the structural evolution of the Sierra de Guadarrama, which is part of the Domain with Recumbent Folds of the CIZ. There, between 75 and more than 200 km to the east of Salamanca, the structure consists of a pile of orthogneissic basement slices (Macaya *et al.* 1991), each of which represents a recumbent fold nappe bounded by mylonitic zones. The crustal shortening associated with this type of tangential tectonics must be very important, but the lower crust is not involved in the slices, though its existence is deduced from gravimetric analysis (Rosales Calvo *et al.* 1977) and from the granulitic enclaves found in lamprophyric dykes and diatremes (Nuez *et al.* 1982, Villaseca *et al.* 1983).

Macaya *et al.* (1991) postulated the existence of a detachment between the hydrous and anhydrous parts of the crust, in order to explain this lack of outcropping. On the other hand, the contrast between the Domains with Recumbent and with Vertical Folds (Fig. 1) suggests the existence of a crustal scale, E-verging shear zone separating both domains, which should have underthrust part of the former below the latter. Whichever the involved mechanisms may be, it is quite possible that substantial amounts of the crust were transferred to the west during the nappe piling. If some of this material was accumulated below the zone studied, it could have contributed to the triggering of the gravitational collapse (Fig. 16b).

CONCLUSIONS

A very important structural element in the region studied is an extensional ductile shear zone, several km thick, that may be described as the Salamanca Detachment Zone. It is probably part of a large family of extensional structures developed in the Central Iberian Zone, which show, as their main characteristics, a direction of movement subparallel to the trend of the orogen and a syn-collisional development. In particular, the one described here is also characterized by the fact that it affects a region of previous steep tectonics, as opposed to the tangential tectonics that usually characterize the former evolution of many gravitationally collapsed orogens. However, the existence of low-dipping compressive shear zones at depth is considered probable on regional grounds.

The finite strain ellipsoid associated to the ductile detachment seems to have been of the plane strain type, and components of rotational and coaxial deformation were probably involved. Coaxial strains can also be identified in the hangingwall, in the form of a sub-

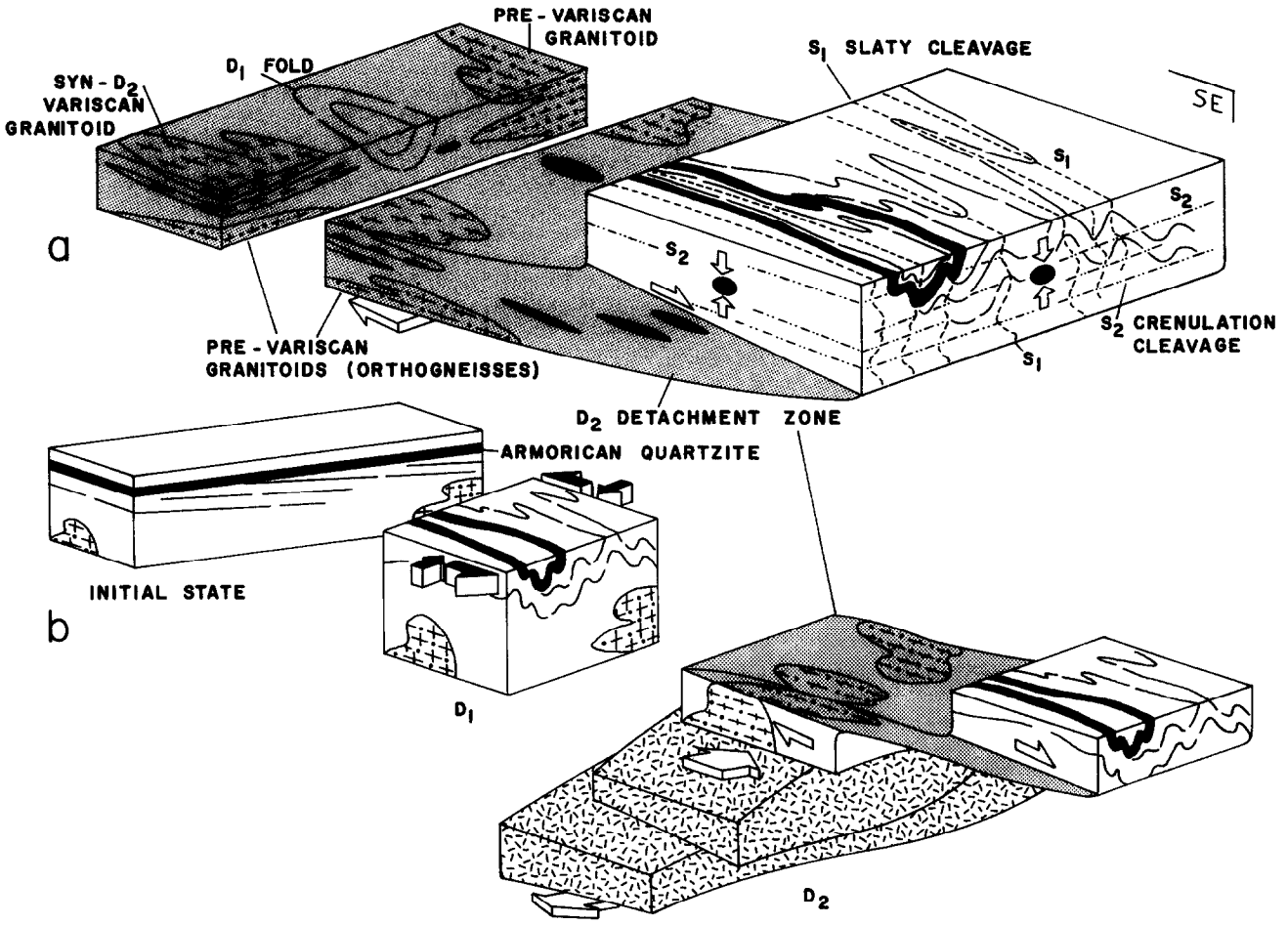

Fig. 16. (a) Structures developed during the D_2 event: extensional shear zone (grey) and horizontal flexures in the hangingwall unit. The ellipses represent D_2 strain and the white arrows the main kinematic components: Rotational deformation in the shear zone and irrotational deformation above. (b) Structural evolution of the area during the main deformation events: D_1 steep tectonics, probably induced by transpression, followed by D_2 gravitational collapse parallel to the trend of the belt. The possible influence in the collapse of lower crustal material (hatched) subcreted from the east is suggested.

horizontal crenulation or crenulation cleavage. The detachment zone is more than 4 km wide. Assuming that the main component of deformation was simple shear and that shear strain equals the maximum calculated 3.5, a translation in the order of 14 km should account for the measured values. This estimation is probably conservative, because the D_2 ellipsoid has been calculated from conglomerates which are supposedly more competent than the dominant schists. However, the translation could not have been too large, as the extension was not enough to place cold sediments on top of the metamorphic rocks, and the hangingwall maintained greenschist facies conditions during the extensional process.

Acknowledgements—Ricardo Arenas is thanked for his help with the study of metamorphism. The drawing of some of the figures by Ignacio Romero Beato and the revision of the English version by Barbara Knowles and Suzanne Marie Irwin are kindly acknowledged. The two reviewers of the manuscript, A. Ribeiro and R. J. Holcombe, contributed greatly to improve the clarity and quality of the final version and are also acknowledged. This paper has been funded by the DGICYT, grant PB 90-0860-C03-02.

REFERENCES

Aller, J., Bastida, F., Ortega, E. & Pérez-Estaún, A. 1986. Aportación al conocimiento estructural del Sinclinal de Almadén. *Bol. Geol. Min. Inst. Geol. Min. España* **97**, 608–621.

Berthé, D., Choukrounc, P. & Jegouzo, P. 1979. Orthogneisses, mylonite and non-coaxial deformation of granites: the example of the South Armorican Shear Zone. *J. Struct. Geol.* **1**, 31–42.

Block, L. & Royden, L. H. 1990. Core complex geometries and regional scale flow in the lower crust. *Tectonics* **9**, 557–567.

Bouchez, J. L., Dervin, P., Mardon, J. P. & Englander, M. 1979. La diffraction neutronique appliquée a l'étude de l'orientation préférentielle de réseau dans les quartzites. *Bull. Minéral.* **102**, 225–231.

Burg, J. P., Iglesias, M., Laurent, Ph., Matte, Ph. & Ribeiro, A. 1981. Variscan intracontinental deformation: the Coimbra-Córdoba shear zone (SW Iberian Peninsula). *Tectonophysics* **78**, 161–177.

Burg, J. P. & Laurent, P. 1978. Strain analysis of a shear zone in a granodiorite. *Tectonophysics* **47**, 15–42.

Chacón, J., Oliveira, V., Ribeiro, A. & Oliveira, J. T. 1983. La estructura de la Zona de Ossa-Morena. *Geología de España. Libro Jubilar J. M. Rios* **1**, 490–504.

Dallmeyer, R. D. & Quesada, C. 1989. Geochronological constraints to the structural evolution of the Badajoz-Cordoba shear belt (Southwest Iberia). *Terra Abstracts* **1**.

Dewey, J. F. 1988. Extensional collapse of orogens. *Tectonics* **7**, 1123–1139.

Dias, R. & Ribeiro, A. 1991a. A kinematic approach to the strain distribution in the Valongo Anticline (Variscan autochthon of Centro Iberian Zone). III Congresso Nacional de Geología. Coimbra, Resumos.

Dias, R. & Ribeiro, A. 1991b. Finite strain analysis in a transpressive regime (Variscan autochthon, northeast Portugal). *Tectonophysics* **191**, 389–397.

Díez Balda, M. A. 1981. La estructura herciniana entre Salamanca y

Sequeros (Zona Centro Ibérica). La superposición de fases y su influencia en la fábrica de las rocas. *Cuad. Geol. Ibérica* **7**, 519–534.

Díez Balda, M. A. 1983. Características del elipsoide de deformación finita ligado a la segunda fase hercínica en áreas meso y catazonales del Sur de la provincia de Salamanca. *Stvdia Geol. Salmanticensia* **18**, 65–80.

Díez Balda, M. A. 1986. El Complejo Esquisto-Grauváquico, las series paleozoicas y la estructura hercínica al Sur de Salamanca. Ed. Universidad de Salamanca.

Díez Balda, M. A., Vegas, R. & González Lodeiro, F. 1990. Central-Iberian Zone. Structure. In: *Pre-Mesozoic Geology of Iberia* (edited by Dallmeyer, R. D. & Martínez García, E.). Springer-Verlag, Berlin, 172–188.

Dunnet, D. 1969. A technique of finite strain analysis using elliptical particles. *Tectonophysics* **7**, 117–136.

Escuder Viruete, J., Arenas, R. & Martínez Catalán, R. (In press). Tectonothermal evolution associated with Variscan crustal extension in the Tormes Gneiss Dome (NW Salamanca, Iberian Massif, Spain). *Tectonophysics*.

Flinn, D. 1962. On folding during three-dimensional progressive deformation. *Q. J geol. Soc. Lond.* **118**, 385–433.

Fry, N. 1979. Random point distributions and strain measurement in rocks. *Tectonophysics* **60**, 89–105.

Galibert, F. 1984. Géochimie et Géochronologie du Complexe granitique de l'antiforme de Morille (Salamanque, Espagne). Unpublished Rapport de stage de D. E. A., Lab. de Géochimie Isotopique, Univ. Montpellier.

Gapais, D., Pêcher, A., Gilbert, E. & Ballèvre, M. 1992. Synconvergence spreading of the Higher Himalaya crystalline in Ladakh. *Tectonics* **11**, 1045–1056.

García Casquero, J. L., Priem, H. N. A., Boelrijk, N. A. I. M. & Chacón, J. 1988. Isotopic dating of the mylonitization of the Azuaga Group in the Badajoz-Córdoba belt, SW Spain. *Geol. Rdsch.* **77**, 483–489.

García de Figuerola, L. C. & Martínez García, E. 1972. El Cámbrico Inferior de La Rinconada (Salamanca, España Central). *Stvdia Geol. Salmanticensia* **3**, 33–41.

Gutiérrez Marco, J. C. & Rábano, I. 1983. Bioestratigrafía de las pizarras ordovícicas en la Sierra de Tamames (Sinclinal de Sequeros-Ahigal de los Aceiteros, prov. Salamanca). *Coloquios Paleont.* **38**, 13–25.

Hansen, E. 1971. *Strain Facies*. Springer-Verlag, Berlin.

Hatcher, R. D. & Hooper, R. J. 1992. Evolution of crystalline thrust sheets in the internal parts of mountain chains. In: *Thrust Tectonics* (edited by McClay, K. R.). Chapman & Hall, 217–233.

Holcombe, R. J., Pearson, P. J. & Oliver, N. H. S. 1991. Geometry of a Middle Proterozoic extensional décollement in northeastern Australia. *Tectonophysics* **191**, 255–274.

Iglesias Ponde de León, M. & Ribeiro, A. 1981. La zone de cisaillement ductile de Juzbado (Salamanca)-Penalva do Castelo (Viseu): Un linéament ancien réactivé pendant l'orogénèse hercynienne? *Comun. Ser. Geol. Portugal* **67**, 89–93.

Jiménez Fuentes, E. 1982. Graptolitos Ordovícicos de la Provincia de Salamanca. *Cuad. Lab. Xeoloxico de Laxe* **3**, 233–240.

Julivert, M., Fontboté, J. M., Ribeiro, A. & Nabais Conde, L. E. 1972. Mapa Tectónico de la Península Ibérica y Baleares E. 1: 1.000.000. Inst. Geol. Min. Esp. Madrid.

Lefort, J. P. & Ribeiro, A. 1980. La Faille de Porto-Badajoz-Cordova a-t'elle controllée l'evolution de l'ocean paléozoique sud-Armoricain? *Bull. Soc. geol. Fr.* **22**, 455–462.

Linares, E., Pellitero, E. & Saavedra, J. 1987. Primeras edades radiométricas en el área Estanno-Wolframífera de Morille-Martinamor (Centro-Oeste de España). *Bol. Geol. y Min.* **93**, 640–646.

Lisle, R. J. 1985. *Geological strain analysis. A manual for the* R_f/Φ *Technique*. Pergamon Press, Oxford.

Lister, G. S. & Davis, G. A. 1989. The origin of metamorphic core complexes and detachment faults formed during Tertiary continental extension in the northern Colorado River region, U.S.A. *J. Struct. Geol.* **11**, 65–94.

Lister, G. S. & Snoke, A. W. 1984. *S–C* Mylonites. *J. Struct. Geol.* **6**, 617–638.

Macaya, J., González Lodeiro, F., Martínez Catalán, J. R. & Alvarez, F. 1991. Continuous deformation, ductile thrusting and backfolding in the basement of the Hercynian orogen and their relationships with structures in the metasedimentary cover in the Spanish Central System. *Tectonophysics* **191**, 291–309.

Martínez Catalán, J. R., Hacar Rodríguez, M. P., Villar Alonso, P., Pérez-Estaún, A. & González Lodeiro, F. 1992. Lower Paleozoic extensional tectonics in the limit between the West Asturian-Leonese and Central Iberian Zones of the Variscan Fold-Belt in NW Spain. *Geol. Rdsch.* **81**, 545–560.

Matte, Ph. 1968. La structure de la virgation hercynienne de Galice (Espagne). *Revue Géol. Alp.* **44**, 1–128.

Matte, Ph. 1988. Décollements in slate belts, examples from the European variscides and the Qin Ling Belt of Central China. *Geol. Rdsch.* **77**, 227–238.

Noronha, F., Ramos, J. M. F., Rebelo, A., Ribeiro, A. & Ribeiro, L. 1981. Essai de correlation des phases de deformation hercyniennes dans le Nord-Ouest pénisulaire. *Leid. geol. Meded.* **52**, 87–91.

Nuez, J., Ubanell, A. G. & Villaseca, C. 1982. Diques lamprofíricos norteados con facies brechoidales eruptivas en la región de la Paramera de Avila (Sistema Central Español). *Cuad. Lab. Xeol. Laxe* **3**, 53–74.

Palacios, T. & Vidal, G. 1992. Lower Cambrian acritarchs from northern Spain: the Precambrian–Cambrian boundary and biostratigraphic implications. *Geol. Mag.* **129**, 421–436.

Passchier, C. W. & Simpson, C. 1986. Porphyroclast systems as kinematic indicators. *J. Struct. Geol.* **8**, 831–843.

Perejón, A. 1972. Primer descubrimiento y descripción de Arqueociatos en la provincia de Salamanca. *Stvdia Geol. Salmanticensia* **4**, 143–149.

Powell, R. & Holland, T. J. B. 1988. An internally consistent dataset with uncertainties and correlations. III. Application methods, worked examples and a computer program. *J. Metamorph. Geol.* **6**, 173–204.

Ramsay, J. G. 1967. *Folding and Fracturing of Rocks*. McGraw-Hill, New York.

Ribeiro, A., Pereira, E. & Dias, R. 1990. Central-Iberian Zone. Allochthonous Sequences. Structure in the Northwest of the Iberian Peninsula. In: *Pre-Mesozoic Geology of Iberia* (edited by Dallmeyer, R. D. & Martínez-García, E.). Springer, Berlin, 220–236.

Rölz, P. 1975. Beiträge zum Aufbau des junpräkambrischen und altpalaeozoischen Grundgebirges in den Provinzen Salamanca und Cáceres (Sierra de Tamames, Sierra de Francia und östliche Sierra de Gata) Spanien (Auszug). *Münster Forsch. Geol. Paläont. Heft* **36**, 1–68.

Rosales Calvo, F., Carbó Gorosabel, A. & Cadavid Camiña, S. 1977. Transversal gravimétrica sobre el Sistema Central e implicaciones corticales. *Bol. Geol. Min. Inst. Geol. Min. España* **88**, 567–573.

Sanderson, D. J. & Marchini, W. R. D. 1984. Transpression. *J. Struct. Geol.* **6**, 449–458.

Schmid, S. M. & Casey, M. 1986. Complete fabric analysis of some commonly observed quartz *c*-axis patterns. In: *Mineral and Rock Deformation: Laboratory Studies—The Paterson Volume. Geophysical Monograph* **36**, Am. Geophys. Union, 263–286.

Simpson, C. & De Paor, D. G. 1993. Strain and kinematic analysis in general shear zones. *J. Struct. Geol.* **15**, 1–20.

Vielzeuf, D. & Holloway, J. R. 1988. Experimental determination of fluid-absent melting relations in the pelitic system. Consequences of crustal differentiation. *Contrib. Mineral. Petro.* **98**, 257–276.

Villar Alonso, P., Escuder Viruete, J. & Martínez Catalán, J. R. 1992. La Zona de Cizalla de Juzbado-Penalva do Castelo en el sector español. *III Congreso Geológico de España y VIII Congreso Latinoamericano de Geología. Salamanca. Simposios* **2**, 446–456.

Villaseca, C., López García, J. A., Nuez, J. & Ubanell, A. G. 1983. Contribución al estudio de los diques camptoníticos heteromorfos con subfacies ocelares y de diatrema asociadas. Sierra de la Paramera de Avila. *Rev. Mat. Proc. Geol.* **5**, 103–118.